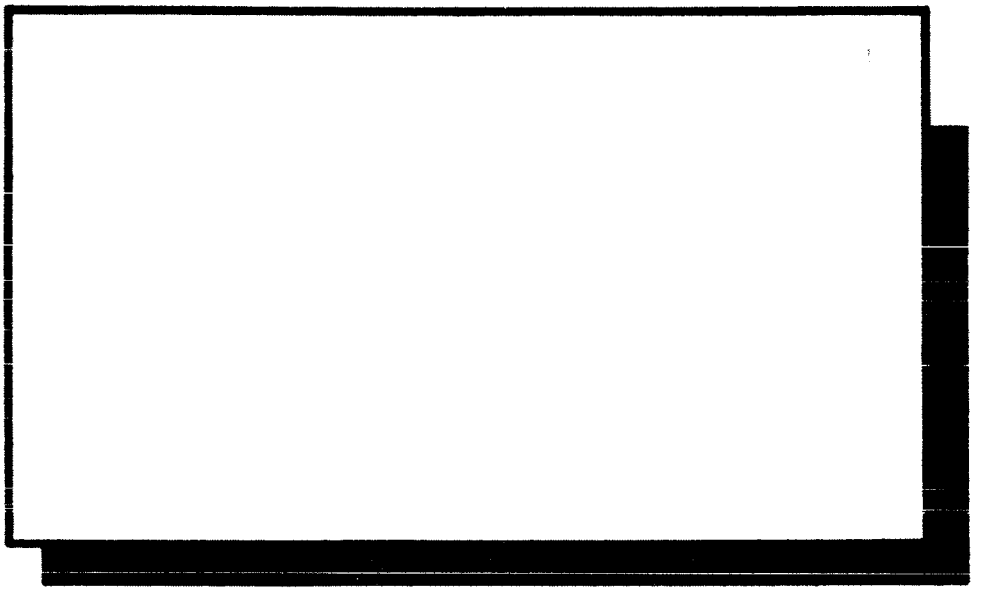

CENTER FOR SPACE RESEARCH
MASSACHUSETTS INSTITUTE OF TECHNOLOGY

Final Technical Report to NASA

for

X-RAY ASTRONOMY EXPERIMENTS FROM SOUNDING ROCKETS

under

NASA Grant NGR 22-009-730

Principal Investigator: Prof. Saul Rappaport

Final Technical Report

to

THE NATIONAL AERONAUTICS AND SPACE ADMINISTRATION

for

X-RAY ASTRONOMY EXPERIMENTS FROM SOUNDING ROCKETS

under

NASA Grant NGR 22-009-730

performed at the

CENTER FOR SPACE RESEARCH

AT THE

MASSACHUSETTS INSTITUTE OF TECHNOLOGY

Principal Investigator: Saul Rappaport

Period covered by the Grant: 08/01/72 to 12/31/86

Date submitted: January 30, 1987

TABLE OF CONTENTS

I. INTRODUCTION

During the past fourteen years, the M.I.T. X-ray Astronomy sounding rocket group has designed, fabricated, and flown five different scientific sounding rocket payloads. These experiment payloads were launched on a total of twelve sounding rocket flights of which only one failed because of rocket problems. Eight of these flights yielded astronomical data that resulted in a total of twelve publications. The bulk of this research was supported by NASA Grant NGR 22-009-730 "X-Ray Astronomy Experiments From Sounding Rockets". The fifth and final experiment payload that was conceived and built under this Grant (the Wide Field Soft X-ray Camera: WFSXC) served as the prototype for the British Wide Field Camera (WFC) experiment to be launched on the ROSAT mission. The five experiment payloads and the results obtained from these experiments are briefly described in the following sections. In the case of the WFSXC, which served principally as an engineering prototype for a major space mission, we present a number of papers witten by our British collaborators which describe the ROSAT Wide Field Camera.

II. LARGE AREA TIMING PAYLOAD

The payload instrumentation consisted of a bank of beryllium window proportional counters, sensitive in the energy range 1.5-10 keV, placed behind $16^\circ \times 16^\circ$ FWHM collimators. The effective area of these detectors ranged between $\sim 600\ cm^{-2}$ and $\sim 900\ cm^{-2}$, depending on the particular flight. The temporal resolution of this system was 1 ms. Additionally, for one of the flights, the instrumentation also contained a rotating modulation collimator system for precise source location measurements. The rotating modulation collimator had a characteristic angular resolution of 2.1' FWHM, and an overall field of view of $16^\circ \times 16^\circ$ FWHM.

The Large Area Timing Payload was flown twice with the following results:

A1. **Aerobee 170 (13.039 UG)**

Launched on September 16, 1972 from the White Sands Missile Range.

A2. Publication resulting from this experiment:

"X-ray Pulse Profile and Celestial Position of Her X-1"
R. Doxsey, H. Bradt, A. Levine, G.T. Murthy, S. Rappaport, and G. Spada
Ap. J. (Letters), **182**, L25 (1973)

B1. **Aerobee 170 (13.105 UG)**

Launched on November 9, 1973 from Woomera, Australia.

B2. Publications resulting from this experiment:

1. "Limits on Rapid X-ray Pulsing in X-ray Binaries"
   G. Spada, H. Bradt, R. Doxsey, A. Levine, and S. Rappaport
   Ap. J. (Letters), **190**, L113 (1974)
2. "Search for Pulsed X-rays from 3U 0833-45 (Vela Pulsar)"
   S. Rappaport, H. Bradt, R. Doxsey, A. Levine, and G. Spada
   Nature, **251**, 471 (1974)

III. BAEZ CONCENTRATOR PAYLOAD

This payload comprised a one-dimensional X-ray concentrator and thin-window proportional counters in the focal plane. The concentrator consisted of 22 nested aluminum plates each coated with Kanigen, a nickel alloy, and highly polished. The reflecting plates were bent in one dimension into parabolic segments all with a common focus and a focal length of 75 cm. The mean reflection angle was 2.5°. Reflectivities, measured at angles from 1° to 7° and at energies between 0.28 keV, and 1.04 keV, were generally within 10% of the theoretical values except near 0.5 keV, where they were lower, probably due to an oxide coating. The angular response of the assembled concentrator was measured optically and was well represented by a triangular function of 0.4° FWHM. The response of the instrument in the nonfocused direction fell to 50% at 5° and 0 at 14° from the optical axis. The two detectors in the focal plane had thin windows of stretched polypropylene, 100 $\pm$ 10 $\mu g\ cm^{-2}$ thick, coated with 45 $\pm$ 10 $\mu g\ cm^{-2}$ of carbon. Each counter had four signal chambers, 4.7 mm in width, which were separated by ground wires. Pure propane at a pressure of 15.8 psia and a total thickness of 0.86 atm-cm was used. Geometrical anticoincidence was provided by a second chamber below the signal chambers.

The Baez Concentrator Payload was flown twice under NASA contract NGR 22-009-730 with the following results:

A1. **Aerobee 170 (13.040 UG)**

Launched on March 30, 1973 from the White Sands Missile Range.

A2. Publications resulting from this experiment:

1. "Discovery of a Central X-Ray Object in the Cygnus Loop"
   S. Rappaport, W. Cash, R. Doxsey, G. Moore, and R. Borken
   Ap. J. (Letters), **186**, L115 (1973)

2. "Possible Detection of Very Soft X-Rays from SS Cygni"
   S. Rappaport, W. Cash, R. Doxsey, J. McClintock, and G. Moore
   Ap. J. (Letters), **187**, L5 (1974)
3. "X-Ray Structure of the Cygnus Loop"
   S. Rappaport, R. Doxsey, A. Solinger, and R. Borken
   Ap. J., **194**, 329 (1974)
4. "Isothermal Blast Wave Model of Supernova Remnants"
   A. Solinger, S. Rappaport, and J. Buff
   Ap. J., **201**, 381 (1975)

B1. **Aerobee 170 (13.104 UG)**

Launched on November 6, 1973 from Woomera, Australia.

B2. Publication resulting from this experiment:

1. "Soft X-Ray Survey of the Large Magellanic Cloud"
   S. Rappaport, A. Levine, R. Doxsey, and H.V. Bradt
   Ap. J., **196**, L15 (1975)

IV. ULTRASOFT X-RAY BACKGROUND PAYLOAD

The detection system in this experiment was designed to have significant effective area at very low X-ray energies (90-280 eV), with little sensitivity to higher energy X-rays, charged particles, or geocoronal ultraviolet. The instrument comprised two concentric paraboloidal X-ray concentrators, and two proportional counters with 1/2 μm polypropylene windows. The X-ray concentrators were constructed by spinning ~ 0.15 inch aluminum around male mandrels. The inside reflecting surfaces were coated with Kanigen, polished and "superpolished". The grazing angles for on-axis rays ranged from 4° to 8°, thus eliminating much of the radiation above 1/4 keV. A series of baffles in the concentrator system eliminated all "straight-though" paths to the proportional counters. At the focal plane of the X-ray concentrators were two identical proportional counters, each with its own propane gas flow system, high-voltage supply, and geometrical anticoincidence anodes, as well as a separated calibration chamber. Each calibration chamber had a small-diameter Be window above which an Al K fluorescent radioactive source was mounted. The gas flow system maintained the counter pressure at 3.5×10^5 dynes cm^{-2} with respect to ambient. Each proportional counter was monitored by pressure transducers in addition to the calibration sources. The window of one counter was coated with a thin carbon layer to provide conductivity

and reduce the sensitivity to ultraviolet light. The other window had a thin boron coating to provide a varied spectral response. The field of view was $\sim 6^{\circ}$ circular with a corresponding solid angle of 0.011 steradians which was nearly independent of X-ray energy.

The Ultrasoft Background Payload was flown three times with the following results:

A1. **Aerobee 170 (13.034 UG)**

Launched on November 16, 1974 from the White Sands Missile Range.

A2. Publication resulting from this experiment:

"On the Ultrasoft X-ray Background"
A. Levine, S. Rappaport, R. Doxsey, and G. Jernigan
Ap. J., **205**, 226 (1976)

B1. **Aerobee 170 (13.108 UG)**

Launched on October 17, 1975 from the White Sands Missile Range.

B2. Publication resulting from this experiment:

"Ultrasoft X-rays From the Southern Galactic Hemisphere"
A. Levine, S. Rappaport, J. Halpern, and F. Walter
Ap. J., **211**, 215 (1977)

C1. **Aerobee 170 (13.050 UG)**

Launched on August 16, 1975 from the White Sands Missile Range.

The scientific objectives of this flight were the same as those ultimately achieved on Aerobee 13.108 (see above). The rocket nosecone failed to eject until severance, when the payload was coming back down into the atmosphere. As a result, no data were obtained and the same payload was flown again two months later.

V. WOLTER IMAGING X-RAY TELESCOPE PAYLOAD

The X-ray detection system comprised an imaging proportional counter at the focal plane of an imaging X-ray telescope. The X-ray telescope, in turn, consisted of two nested paraboloidal -hyperboloidal mirrors of the Wolter I type with outer dimensions 40 cm (diameter) $\times$ 80 cm (length). The focal length of 114 cm corresponded to a focal-plane scale of 3.0 arc min mm^{-1}. Each mirror was constructed of two segments ($\sim$ 40 cm in length) which were machined from solid ingots of forged aluminum on a conventional numerically controlled lathe. The reflecting surfaces

were coated with electroless nickel and then polished with no figuring beyond that of the original machining. X-rays reflected from the mirror were focused on the thin (1 μm polypropylene) window of the imaging detector. Below this window is an electron drift region and a multiwire proportional chamber array; beneath this was an anticoincidence counter. The complete detector was filled with 75% methane amd 25% argon at atmospheric pressure. The multiwire chamber comprised an anode with a 2 mm wire pitch and two cathodes, one 4 mm above the anode, the other 4 mm below. Both cathodes had 1 mm wire pitch; the wires on the lower one running perpendicular to those on the upper. Each wire on the cathode was separated from the adjacent wires by a fixed resistance, so that a complete cathode formed an RC transmission line.

The Wolter Imaging X-ray Telescope Payload was flown twice and (i) yielded the first true X-ray images of supernova remnants and (ii) represented the first use of a Wolter X-ray telescope in non-solar astronomy. Specifically, the following results were obtained with this payload:

A1. **Astrobee (25.021 UG)**

Launched on July 26, 1977 from the White Sands Missile Range.

A2. Publication resulting from this experiment:

"X-ray Image of the Cygnus Loop"
S. Rappaport, R. Petre, M. Kayat, K. Evans, G. Smith, and A. Levine
Ap. J., **227**, 285 (1979)

B1. **Astrobee (25.023 UG)**

Launched on March 8, 1978 from the White Sands Missile Range.

B2. Publication resulting from this experiment:

"X-ray Images of Puppis A and IC 443"
A. Levine, R. Petre, S. Rappaport, G. Smith, K. Evans, and D. Rolf
Ap. J. (Letters), **228**, L99 (1979)

VI. WIDE FIELD SOFT X-RAY CAMERA PAYLOAD

A. Payload Description

The X-ray camera consisted of wide-field (6°) imaging X-ray optics with a microchannel plate detector at the focal plane. The telescope optics comprised three nested mirrors that were basically of the Wolter I type. The image was recorded with a 50 mm diameter microchannel plate detector with 25μm channel-pore size. The energy bandpass (50Å-250Å) was determined by two fixed

filters in the focal plane, each of which covered one half of the imaging detector. The image readout was accomplished via a resistive sheet, on which the charge, generated when an X-ray entered the detector, was deposited, and four amplifiers. Aspect was provided by a 16 mm star camera to $\sim$ 1' accuracy. A schematic of the payload is shown in Figure 1 and a photograph of the Black Brant 21.069 payload is shown in Figure 1a.

B. Flights of the WFSXC

The first flight of the Wide Field Soft X-Ray Camera (**Astrobee 25.040**) took place on October 16, 1981, from the White Sands Missile Range. The Astrobee F rocket vehicle and all support equipment (e.g., attitude control system and telemetry) functioned normally. Based on the "quick-look" data, it appeared that useful astronomical data had been collected. More detailed analysis of the flight data, and laboratory tests indicated that, in fact, coronal discharge had occurred within the detector vacuum housing throughout the flight. Apparently, the lid to the vacuum housing leaked on launch, which resulted in sufficiently high pressure to initiate corona when the high voltage was turned on. This corona effectively shut the experiment down. In response to this problem we made several modifications to the payload to prevent coronal discharge in future flights. These included: (i) a rebuilt vacuum housing with welded stainless steel construction to allow it to better withstand launch vibration, and (ii) switches, for use in sending real-time commands from the ground, to turn the detector high voltage on and off.

The second flight of the Wide Field Soft X-Ray Camera took place on November 1, 1982, from the White Sands Missile Range. Aside from the changes in the vacuum housing discussed above, the most important modification to the payload was the use of a CsI photocathode surface for the microchannel plate detector. The **Black Brant rocket (21.069)** and most of the support systems functioned normally. The attitude control system, however, was not programmed properly and four of our six celestial targets were missed. There was another problem with the experiment, however, which was of a more profound nature. The background counting rate was sufficiently high that our telemetered X-ray position channels were nearly saturated. From this we inferred that the microchannel plate was detecting $\sim 10^5$ events sec^{-1}. Careful analysis of the flight data and extensive post-flight laboratory tests indicated that the high count rate may have been caused by a high residual presure within the payload at altitude. The payload was then modified by adding (i) two ejectable doors in the payload cylinder to ensure proper evacuation of the payload at altitude, and (ii) a motorized lid to the vacuum housing to provide a more secure vacuum seal on launch and to allow the lid to be closed at the end of the flight so that the detector and filter could be recovered in good working order.

The third, and most recent flight of the WFSXC occurred on March 18, 1985, at the White

Sands Missile Range (**Black Brant 21.070**). The payload achieved a good altitude of 213 km, and the attitude control, telemetry, and recovery systems all functioned nominally. The rocket payload was preprogrammed to scan slowly across five selected soft X-ray sources: HZ 43 and EG 187 (hot white dwarfs), Mkn 421 (a BL Lac object), H1504+65 (a HEAO A2 soft X-ray source), and σ Cor Bor (an RS CVn star). The flight scan paths are shown in Figures 2a, 2b, and 2c. The total area of the sky scanned was $\sim$ 300 square degrees with a potential exposure of $\sim$ 10-15 sec on each source. The total background counting rate from the microchannel plate detector was $\sim$ 50 sec^{-1} - as small a value as could be expected with a large 40-mm diameter MCP detector, a 6° diameter field of view, and ultra-thin filters. The only obvious malfunction involved the aspect camera which was defocused on launch and yielded only very limited aspect information.

The flight data were subjected to a thorough search for any evidence of X-rays from celestial point sources. No such evidence was found in either the overall count rate data or in sky images produced from the data recorded during slow scans across the candidate sources. The sky images (Figures 3a -3d) were made by projecting each detected event onto the sky according to its location in the detector while compensating for the motion of the X-ray camera under the assumption that its optical axis correctly followed the preprogrammed sequence of manuevers.

The hot white dwarf source HZ 43 was included as a calibration target. We estimated that $\sim$ 70 events should have been detected from HZ 43 if the telescope axis had scanned directly across the source. However, fewer than 10 X-ray events were actually detected from this source. The intensities and spectra of the other four targets were not known sufficiently well to permit an accurate estimate of their expected count rates.

Two factors may have contributed to the failure to detect any sources. First, the mirror reflectivity may have been less than that used in our estimates of the expected count rates. The inherent difficulty in making measurements in the 100 - 200 Å band made the reflectivities in this waveband difficult to calibrate properly. Secondly, the sources may have passed through the field of view of the detector at angles up to 2-3 ° from the optical axis. Such an occurence is within the range of expected performance of the rocket attitude control system. For an off-axis angle of 2.5°, the count rate from a source is reduced by nearly a factor of three from the on-axis intensity.

C. The British Wide Field Camera Experiment on ROSAT

Starting with our work on the Wolter Imaging X-ray telescope (Sect. V), we have had an ongoing collaboration with the X-ray astronomy group at the University of Leicester. After two successful flights of this payload, we decided that, because of the impending launch of the Einstein satellite, we should develop a new sounding rocket payload with properties that would be complementary to those of Einstein. Our sounding rocket proposal of May 1979 contained a

description of a new proposed payload centered around a wide field soft X-ray camera that would operate in the wavelength range ~ 80 Å to 250 Å. The collaborative effort with the University of Leicester is described therein. M.I.T. was to develop the payload structure, the wide-field X-ray mirror, and the processing electronics, while the University of Leicester was to prepare the large-area microchannel plate detector with its preamplifier system. This is, in fact, how the collaboration did proceed during the development, testing, and three subsequent flights of the WFSXC payload (see Sect. VI.B).

Shortly thereafter, in December 1979, the German Ministry of Research and Technology sent a letter to the ESA member states inviting participation in what was then known as the Robisat mission. In response to this announcement of opportunity, the University of Leicester submitted a proposal for an ancillary experiment on Robisat, which was essentially a scaled-up version of the WFSXC. Their original proposal of early 1980 is included as Appendix A. Note, in particular, that the University of Leicester stated that that they were submitting the proposal "in collaboration with the Center for Space Research, MIT" (see the cover page of their proposal). We recognized, however, that this would carry no legal obligations for NASA. Only ESA member states were eligible to submit proposals for the Robisat ancillary experiment.

The Leicester proposal was successful, and ultimately a consortium of British X-ray astronomers (from the University of Leicester, Mullard Space Science Laboratory, University of Birmingham, Imperial College of Science and Technology, and the Rutherford Appleton Laboratory) received approval from the British Science Research Council to participate in the Wide Field Camera experiment on what had become the ROSAT mission. ROSAT is now scheduled for launch in ~ 1991. A photograph of ROSAT during a calibration run is shown in Figure 4. The WFC instrument, which is a direct descendant of our WFSXC sounding rocket experiment is described in the following paragraphs and in Appendices B through E.

D. Description of the Wide Field Camera

The ROSAT satellite will carry a large X-ray telescope and an XUV telescope - the Wide Field Camera (hereafter WFC) - with a geometrical collecting area of 511 cm^2. The primary scientific objective of the WFC is to perform an all-sky survey in the XUV wavelength band 60 - 200 Å. The WFC complements the main X-ray telescope by extending the wavelength range well into the XUV band. The WFC will perform an all-sky survey in this band, to locate point sources to better than one arc minute, map extended sources and the XUV background, and by use of selected filters, perform broadband photometry.

The WFC detection system consists of three nested gold-coated aluminum mirrors with a microchannel plate detector at their common focus. A schematic of the telescope is shown in Figure

5. A focal-plane turntable is used to select one of two identical detector assemblies. Any one of 8 filters, mounted on an aperture wheel in front of the detectors, can be selected to define the wavelength passbands and suppress geocoronal background radiation which would otherwise saturate the detector count rate. A baffle assembly mounted in front of the mirrors excludes scattered solar radiation from the mirror apertures and provides thermal decoupling between the mirrors and space. A UV calibration system, mounted on the mirror support, permits in-flight monitoring of detector gain drifts and thermally induced misalignment of the telescope axis. Two particle detectors measure the background charged particle flux and provide a signal to switch off the XUV detectors during ROSAT's passage through the high background regions of the South Atlantic Anomaly and the North and South Auroral zones. Background electrons reflected by the mirrors into the telescope volume are deflected away from the detector aperture by a magnetic diverter system. A schematic of the overall WFC experiment is shown in Figure 6.

During the all-sky survey, two filters will be used, covering the waveband from $\sim$ 60 Å up to 200 Å. For pointed observations, additional filters will be available to extend the spectral response to longer wavelengths.

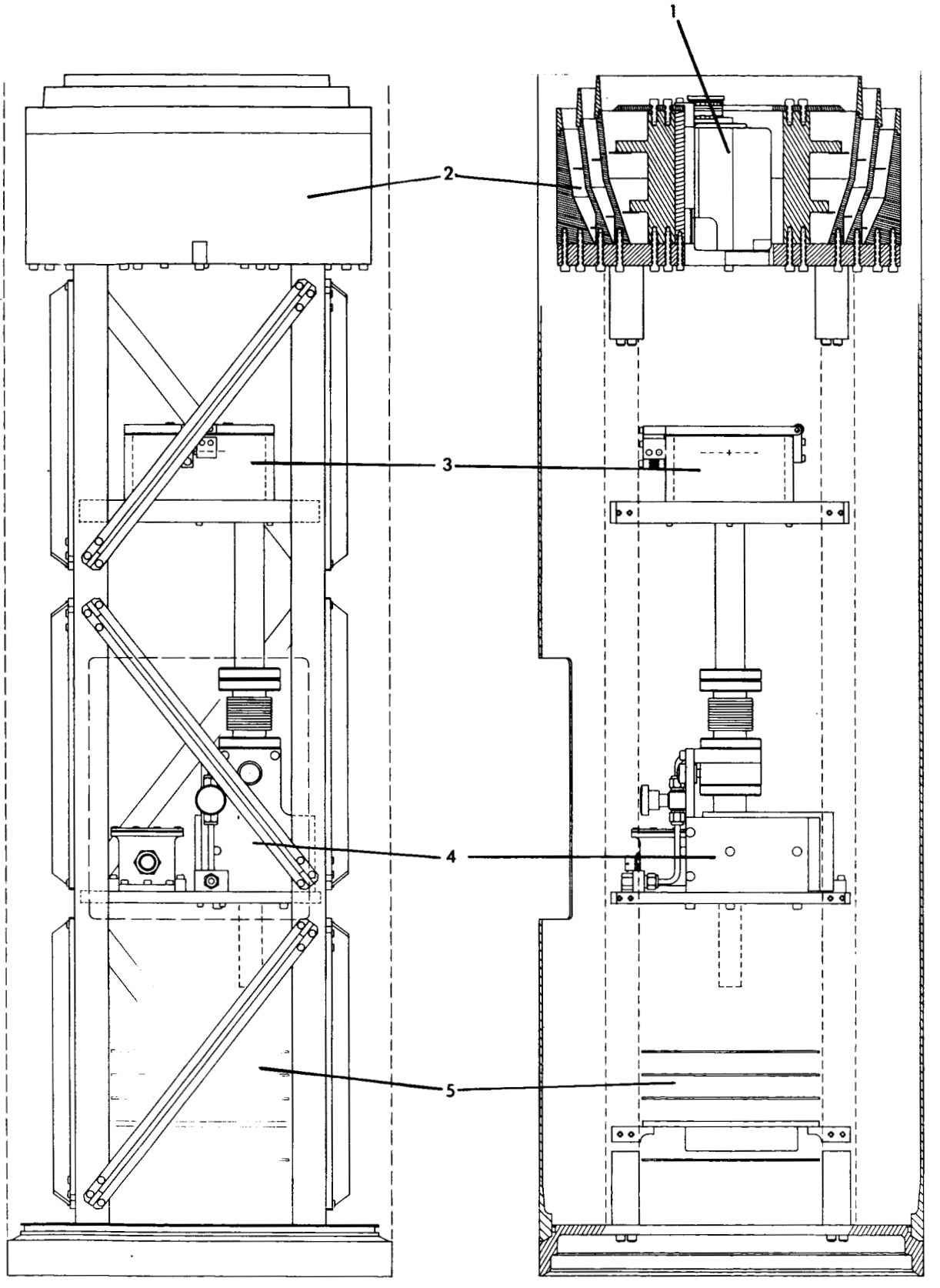

Figure 1: Schematic of the Wide-Field Soft X-Ray Camera payload. Key components include: (1) aspect camera, (2) nested telescopes, (3) detector vacuum housing, (4) ion pump, (5) electronics boards.

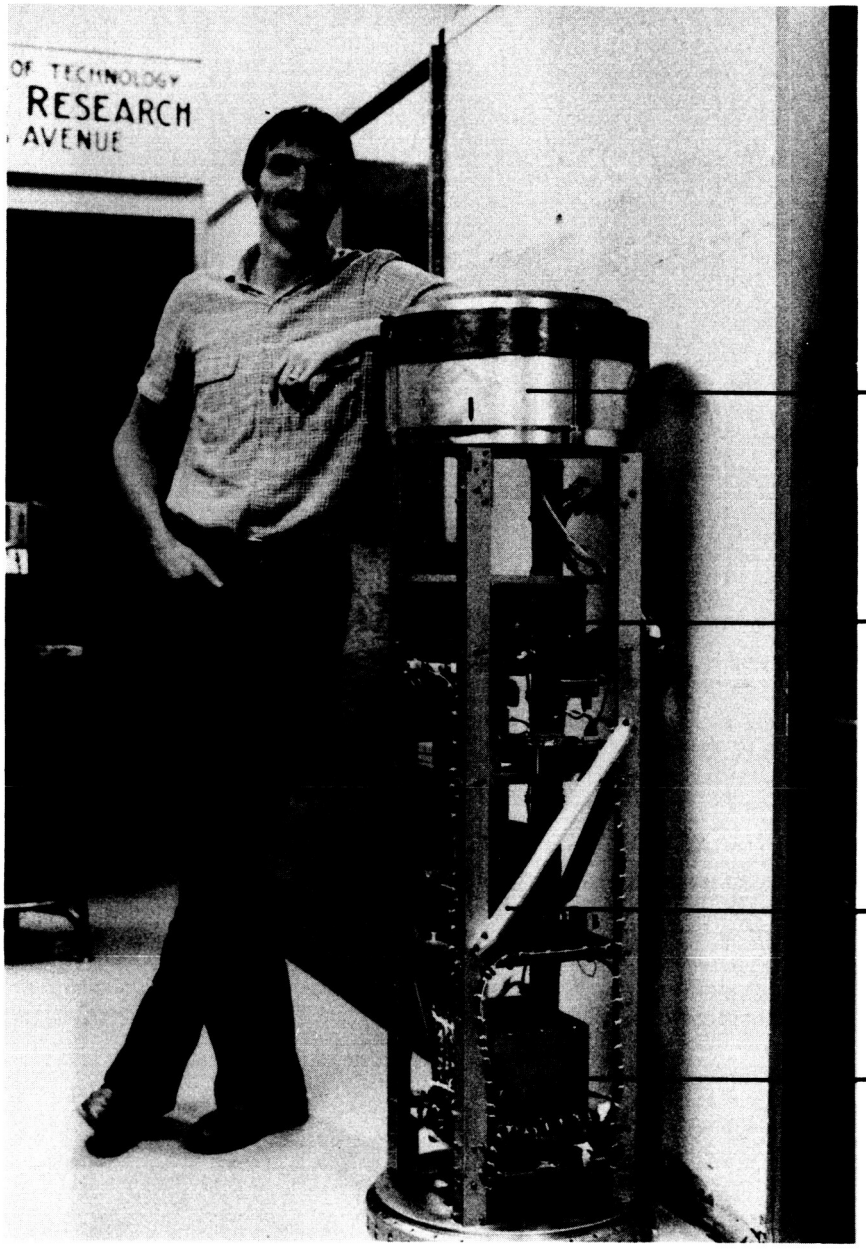

Figure 1a: Wide-Field Soft X-Ray Camera Payload

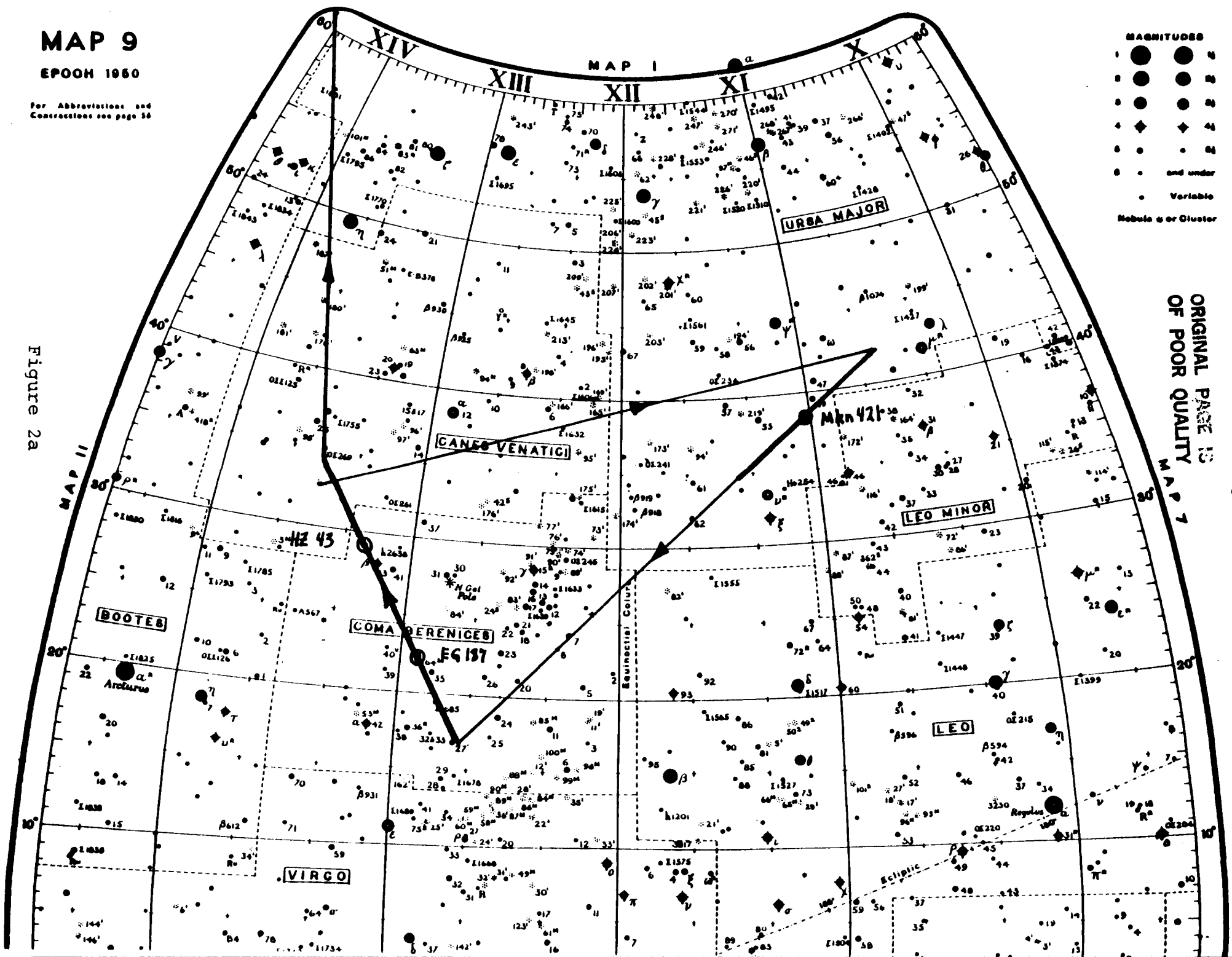

Figure 2a

ORIGINAL PAGE IS
OF POOR QUALITY

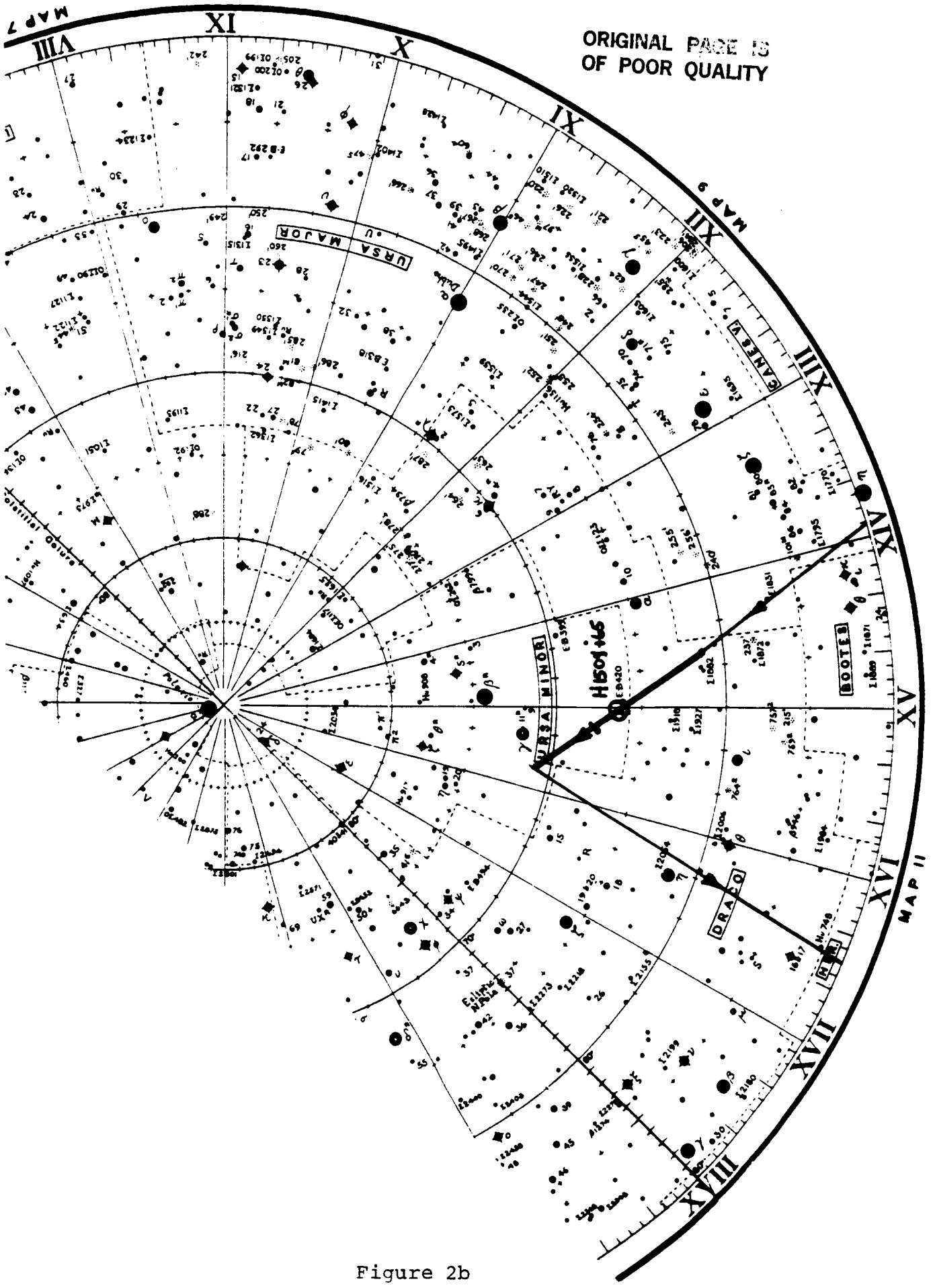

Figure 2b

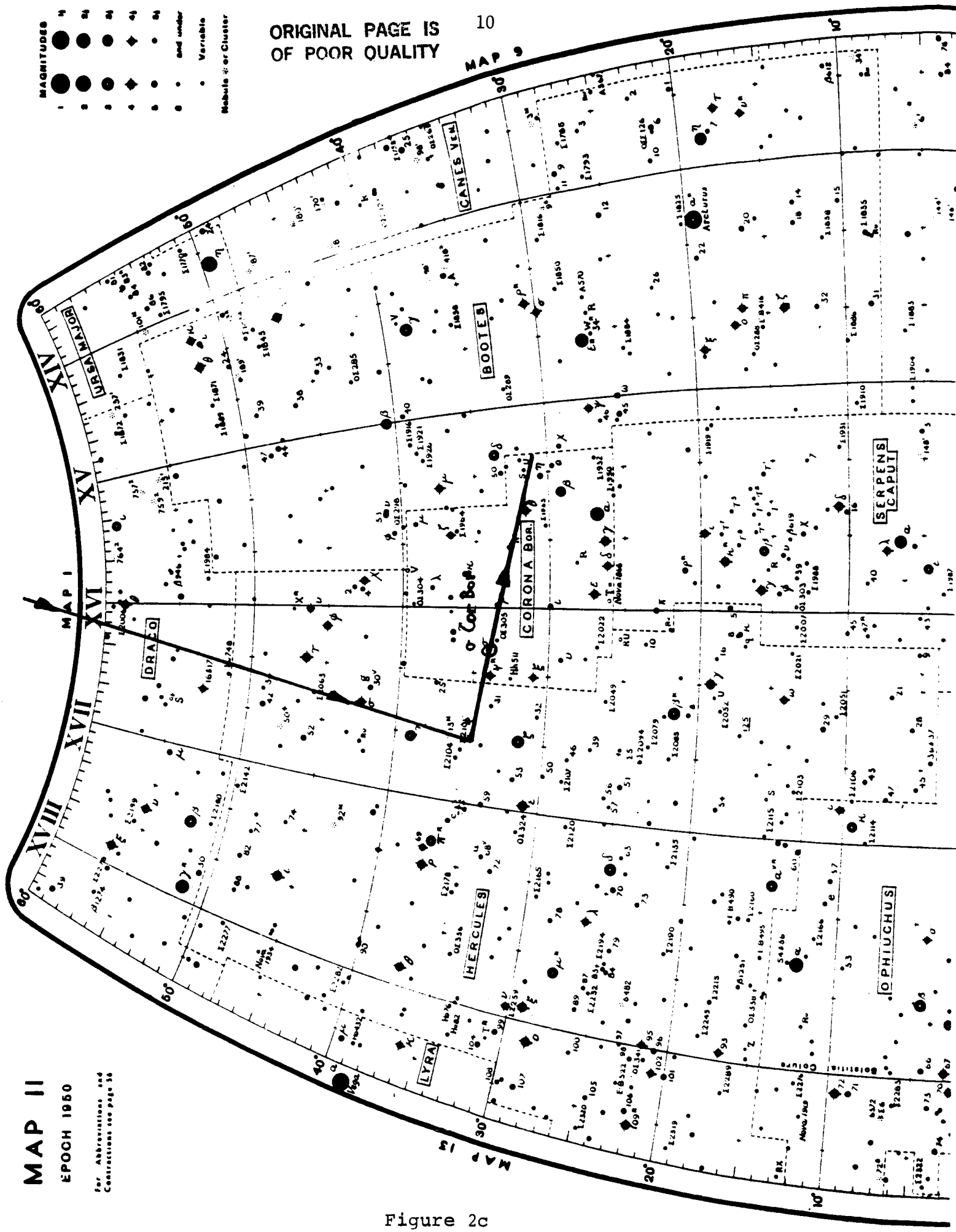

Figure 2c

SCAN 1

Black Brant 21.070

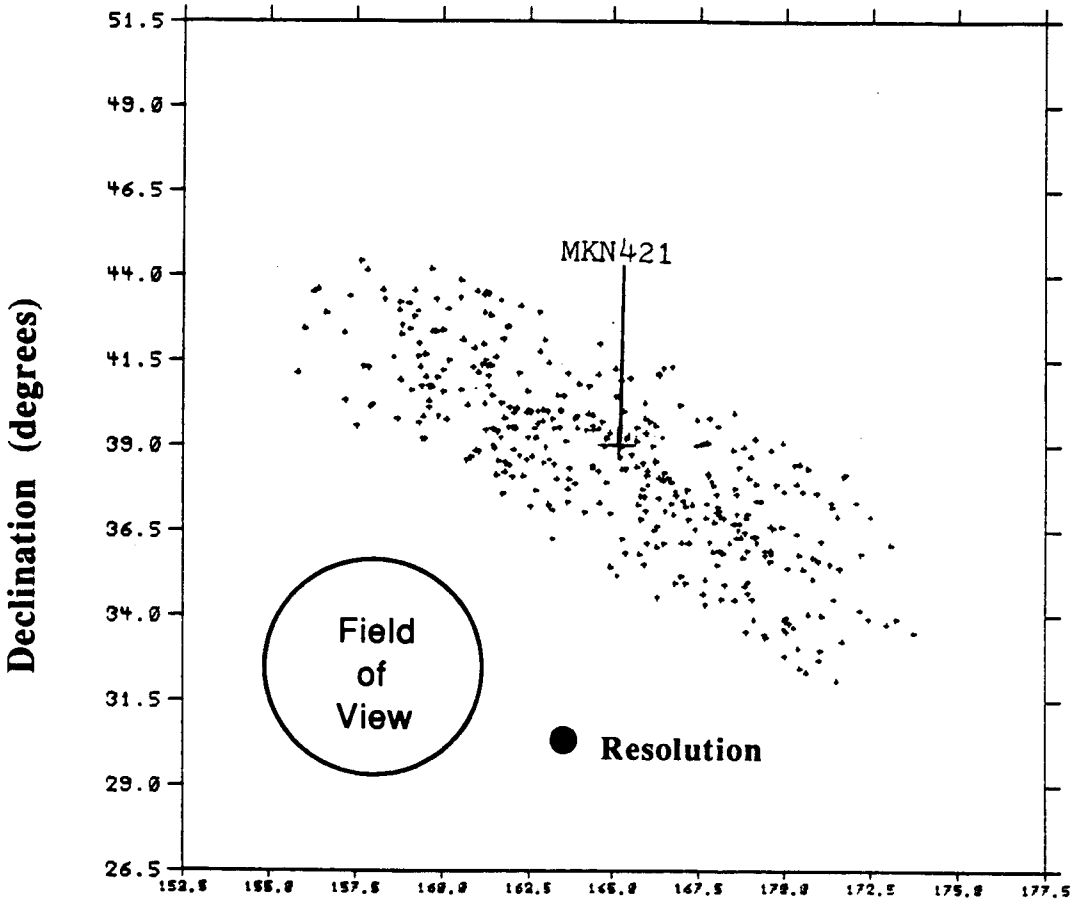

Figure 3a

SCAN 2

Black Brant 21.070

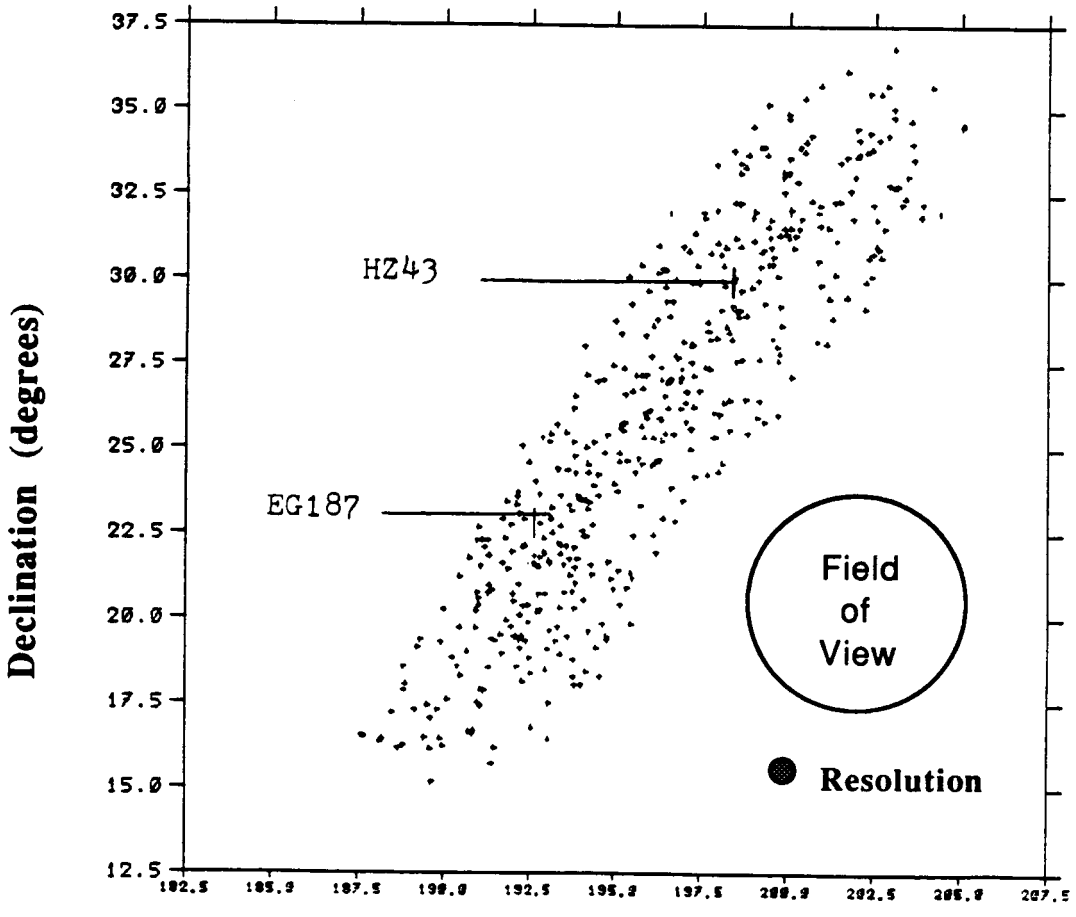

Figure 3b

SCAN 3

Black Brant 21.070

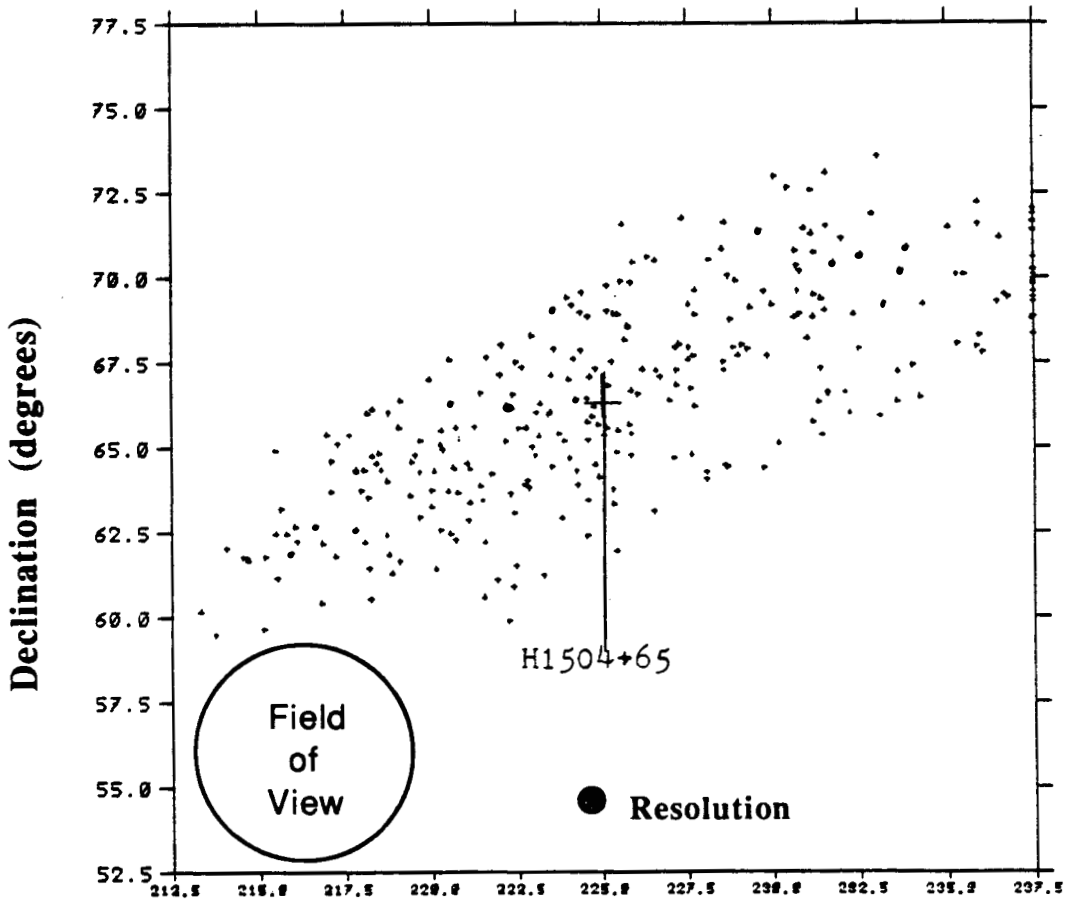

Figure 3c

SCAN 4

Black Brant 21.070

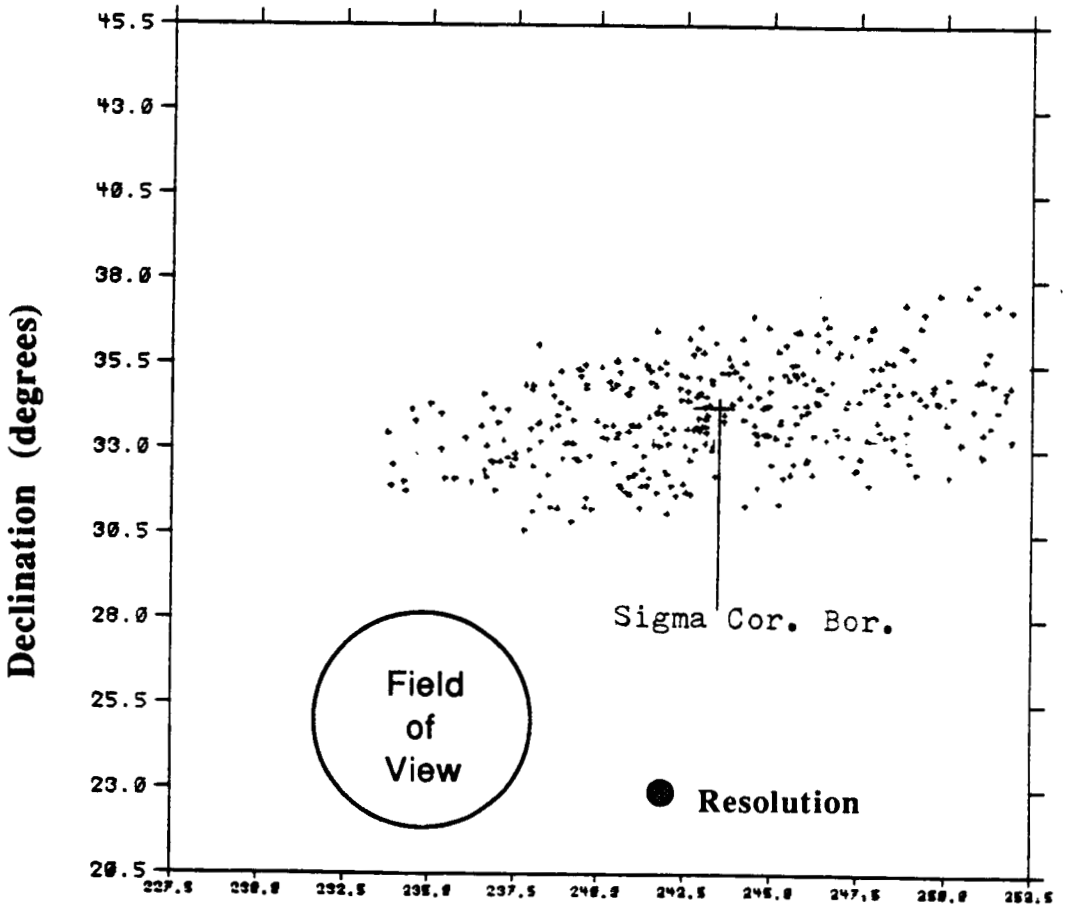

Figure 3d

	XRT	WFC
Overall Length (Door Closed)	3920 mm	1280 mm
Focal Length	2400 mm	525 mm
Diameter	1130 mm	700 mm
Mass	1410 kg	128 kg
Field of View	± 1°	± 2.5°
Power Consumption		
– Sun Phase	170 W	57 W
– Eclipse	70 W	32 W
Spectral Range	0.1 – 2 keV	0.04 – 0.2 keV

Telescopes Performance Parameters

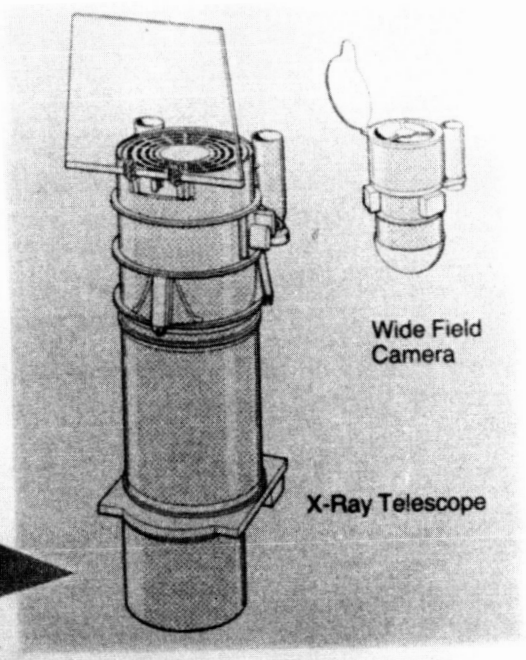

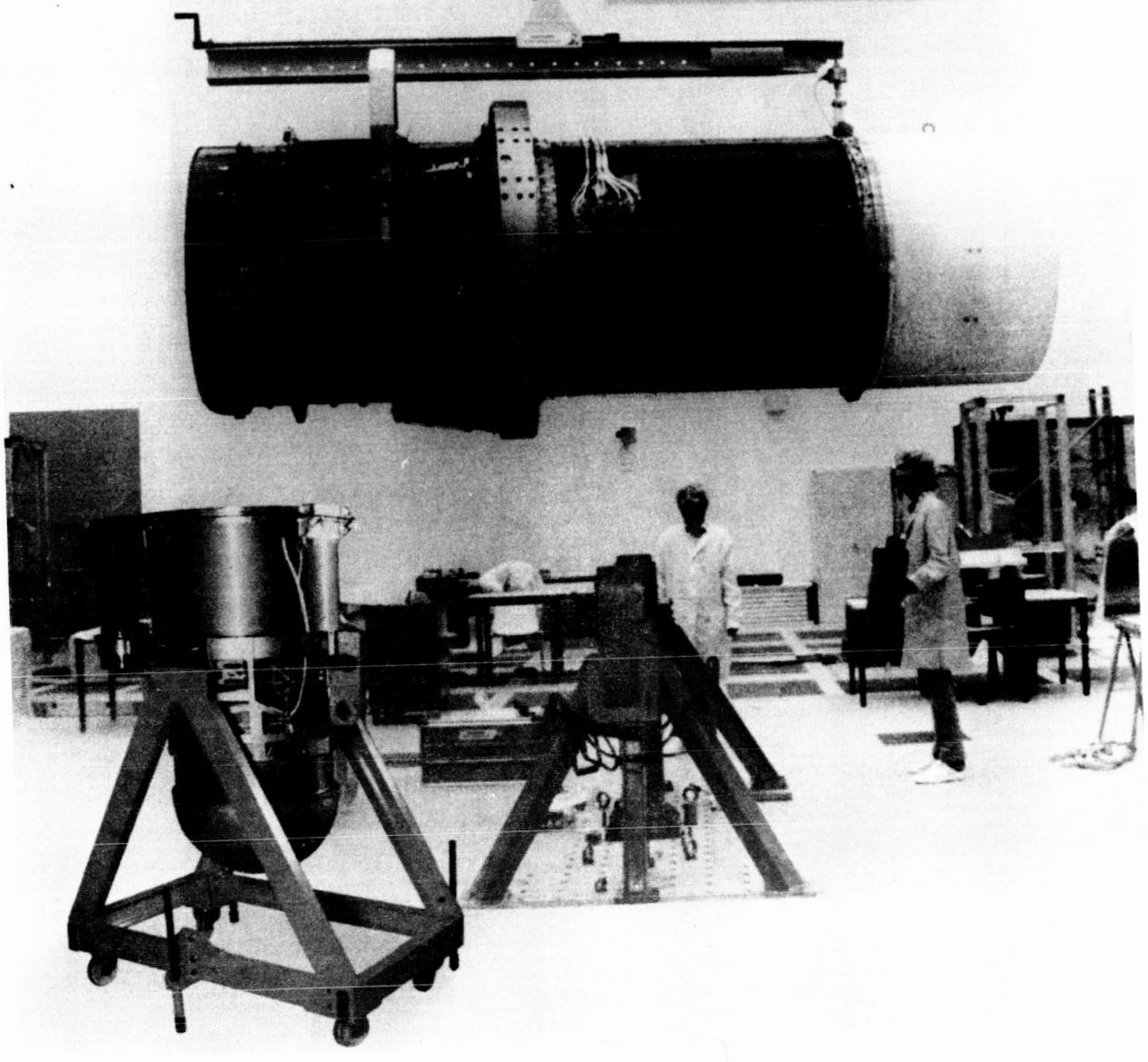

Figure 4

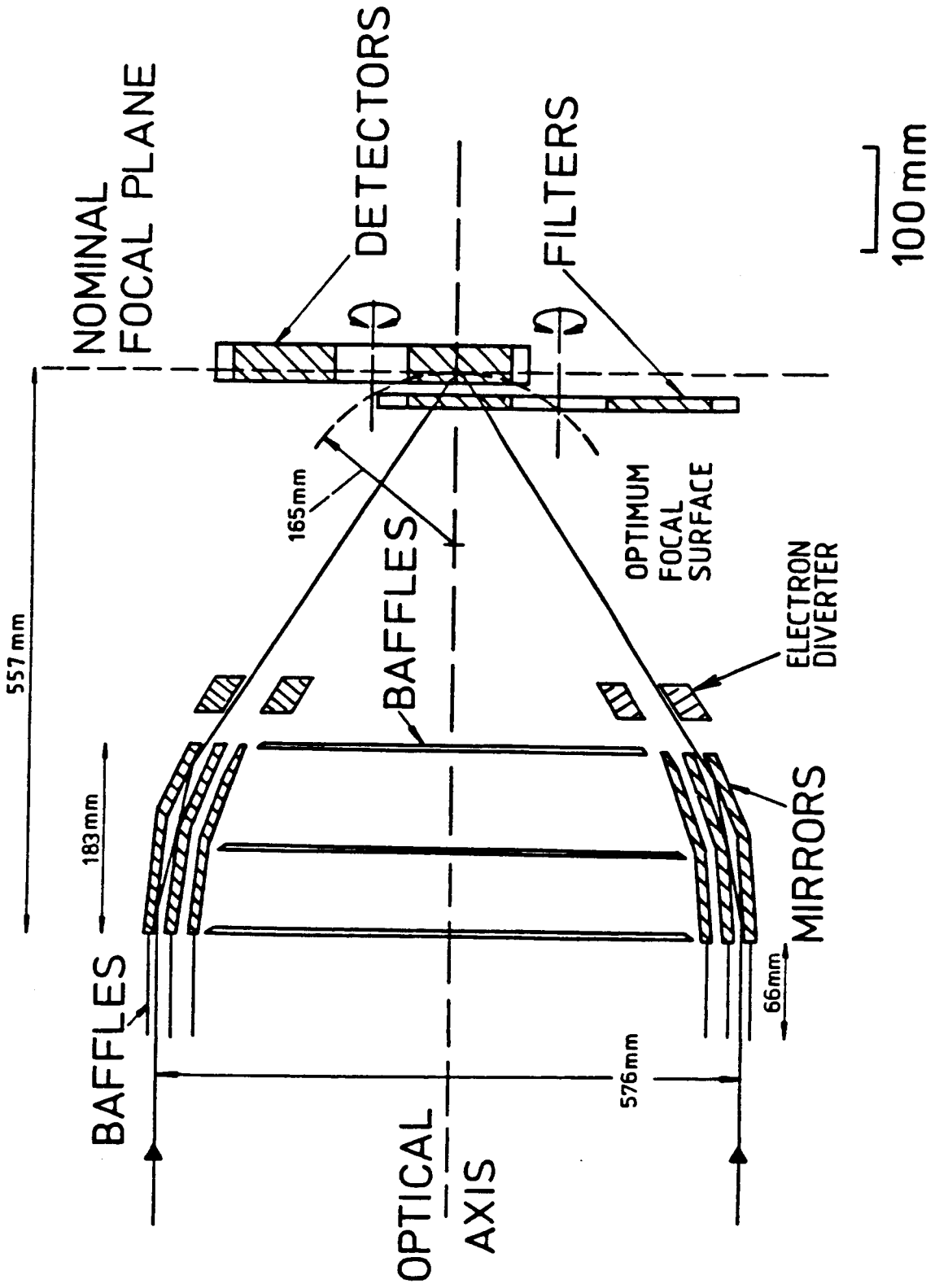

Schematic diagram of the WFC telescope

Figure 5

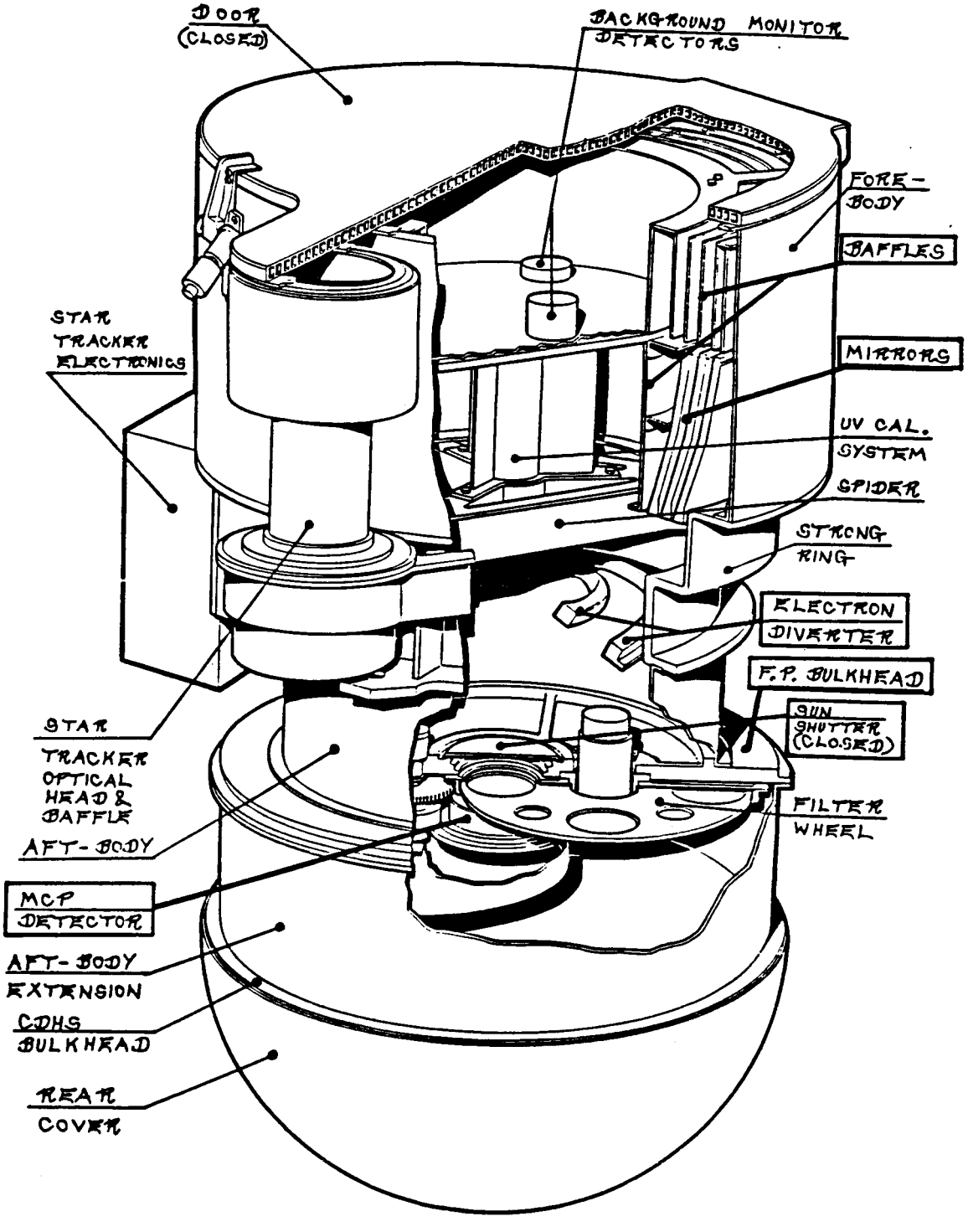

Arrangement of the WFC

Figure 6

APPENDIX A

ORIGINAL UNIVERSITY OF LEICESTER PROPOSAL
for
THE WIDE FIELD CAMERA
on
ROSAT

K A Pounds

A Proposal to the Science Research Council

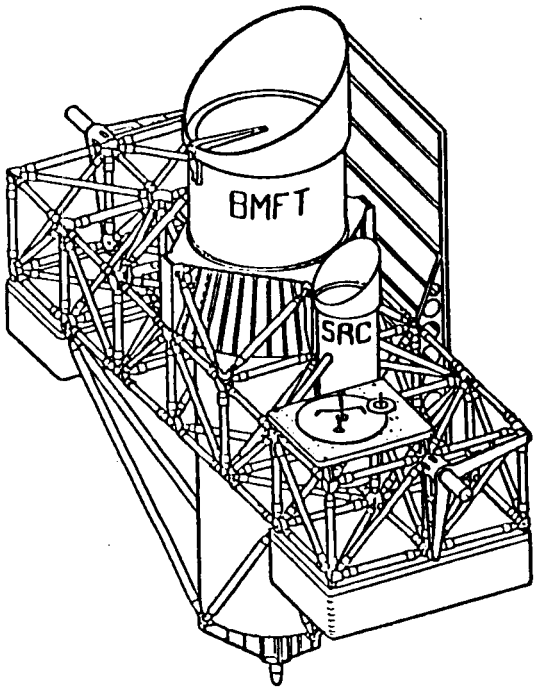

for a

WIDE FIELD SOFT X-RAY CAMERA

to be flown as an ancillary experiment on
the German satellite Robisat.

Submitted by the X-ray Astronomy Group, University of Leicester,
in collaboration with the Center for Space Research, MIT.

Contents

1. Summary

This proposal is in response to the letter from Dr Strub of the German Ministry of Research and Technology to ESA member states (3-12-1979) inviting participation in the X-ray astronomy satellite, Robisat. Following informal discussions with the X-ray Astronomy group at the Max Planck Institut in Garching, we believe the proposal to be strongly complementary to the main Robisat payload which comprises an 80 cm aperture Wolter I X-ray telescope. Our Wide-Field Soft X-ray Camera is based on an instrument developed jointly with MIT and shortly to be flown in the first of a series of NASA Astrobee rocket flights. The baseline proposal is to fly a refurbished version of the rocket camera. However, a number of modifications which would be examined during a Phase B study are also listed in the proposal.

The main Robisat X-ray telescope is intended to provide the first deep all-sky survey using X-ray optics and will extend more than two orders of magnitude below the limits of the Uhuru and Ariel V surveys. The energy range covered will be $\sim 2 - 0.15$ keV (6-80 Å). Our Wide-Field Soft X-ray Camera would extend the range of the Robisat survey to 0.25 - 0.05 keV (50 - 250 Å). Both in respect of the greatly extended energy range and the all-sky coverage the combined Robisat mission would form a powerful follow-up to the current highly successful Einstein Observatory.

The proposed Soft X-ray Camera would allow the study of a wide range of astrophysical objects. These include (i) stellar sources, particularly those with temperature components in the range $10^5 - 10^6$K, (ii) faint extended objects (e.g. supernova remnants, clusters of galaxies, lobes of giant radio galaxies) and (iii) the diffuse soft X-ray background.

The experimental approach utilises a wide field (8° diameter) soft X-ray imaging camera. The camera comprises a grazing incidence X-ray telescope with a microchannel plate detector at the focal plane. The angular resolution of the camera will be $\sim 2'$ over the central 4° diameter region and $\sim 5'$ over the remainder of the 8° field. Photon energy discrimination is provided by thin-film filters which divide the wavelength range, 50Å - 250Å, into several intervals. An objective grating, and filters which extend the wavelength coverage into the EUV, would be optional for future missions.

We at the University of Leicester and MIT are jointly developing a Wide-Field Soft X-ray Camera for use in sounding rocket experiments. (This work is supported by the Science Research Council in the U.K. and by NASA Sounding Rocket funds in the U.S.). It is anticipated that this instrument will be operational by July 1980 and will be flown at least three times during the period to the end of 1981. Design modifications necessary for up-grading for Robisat would include a solar protect system, a passive thermal blanket, and probably a high capacity tape recorder.

The Wide-Field Soft X-ray Camera would be mounted to view along an axis parallel to the main Robisat telescope. Scanning (survey) and pointing requirements will be common and aspect will be provided from the main Robisat attitude sensors. The initial mission plan calls for a 6 month all-sky survey followed by 18 months of individual source and source-field studies. The latter observations will support a substantial guest investigator programme. The baseline Robisat mission proposes data storage on a high capacity tape recorder with transmission each day to the Weilheim ground station. The possibility of using an additional ground link to Winkfield (at least for the U.K. experiment) is being considered.

2. Scientific Objectives

Most of our knowledge of the X-ray sky has been obtained in the $\sim 0.5 - 20$ keV region of the spectrum from extensive satellite observations, including those of Uhuru, OSO-7, Copernicus, ANS, Ariel V, SAS-3, OSO-8, HEAO-1 and most recently the Einstein Observatory. There are presently several thousand X-ray sources that have been detected; these include X-ray binaries, supernova remnants, flare stars, radio pulsars, ordinary galaxies, galaxies with active nuclei, quasars and clusters of galaxies.

Exploration of the X-ray sky has also been extended to softer X-ray wavelengths 10A - 80A ($\sim$ 150eV - 1 keV), by means of numerous sounding rocket experiments, by several modest-size satellite experiments (ANS, Copernicus, SAS-3, OSO-8), and most recently by HEAO-1 and Ariel VI. Although the soft X-ray sky has not yet been as well studied as at higher energies, a rich variety of sources has been discovered. These include (i) supernova remnants (see Figure 1); (ii) stellar sources such as hot white dwarfs (e.g. HZ43[4] -see Figure 2; Feige 24[5]), dwarf novae (e.g. SS Cyg[6,7], U Gem[8,9], AM Her[10] - Figure 3), flare stars (Prox Cen[11], UV Ceti[12]), stellar coronae[13] (Capella[14,15,16], Sirius [16]); (iii) the soft X-ray background[17,18,19] (Figure 4); (iv) extragalactic objects, such as clusters of galaxies[21,22] and BL Lac objects (e.g. Mkn 421[23]). Investigation of the above classes of objects, in selected regions of the sky, is now being greatly accelerated with the advent of the Einstein Observatory (sensitive in the energy range $\sim$0.2 - 4 keV).

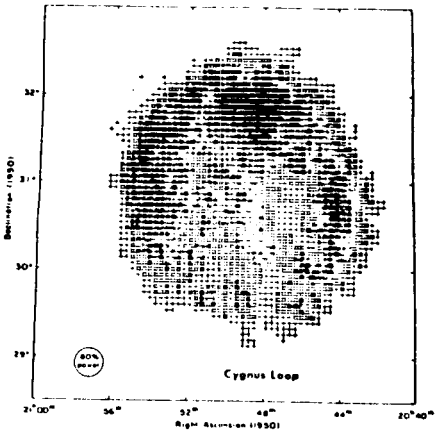

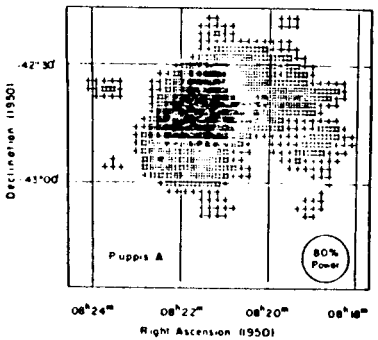

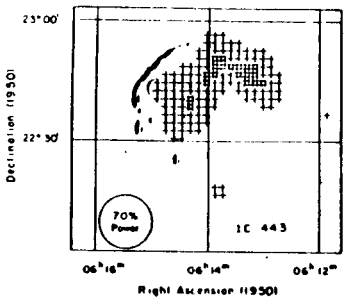

Figure 1 - MIT and U. of Leicester x-ray images of the Cygnus Loop, Puppis A and IC443 supernova remnants in the wavelength range 10Å-80Å(1,2). These represent the first x-ray pictures of supernova remnants recorded with an imaging x-ray telescope. These are also the first celestial x-ray images (extrasolar) produced with a Wolter-type telescope.

The sky is largely unexplored at very soft X-ray energies below ~0.2 keV. The Apollo-Soyuz mission, which yielded ~20 pointed observations (0.2% of the sky)[24], resulted in the discovery of at least four sources in this range: Feige 24[5], Prox Cen[11], HZ43[4] and SS Cyg[8], the latter two of which had been detected previously at somewhat higher energies. These detections, and other recent studies of the interstellar medium, strongly indicate that these very soft X-rays can be detected from significant distances from the earth[25,26,27]. A graph, summarising the distance to which soft X-rays can penetrate the interstellar medium, for reasonable densities ($0.03 < n < 0.2$ within ~100 pc of the sun), is given in Figure 5. At 100Å (0.12 keV) for example, it is possible to "see" out of our galaxy at high galactic latitudes.

The wealth of spectacular results accumulated in the past year and a half by the Einstein Observatory has ushered in a new era in X-ray astronomy. By the end of its three-year lifetime, the Einstein observatory will have imaged and/or measured the spectrum of virtually all known or suspected cosmic X-ray sources, discovered thousands of new sources, and provided the most sensitive look at a portion of the celestial sphere. The primary limitation of Einstein is that during its lifetime the relatively small fields of view of the HRI and IPC ($\sim 1/3^\circ + \sim 1^\circ$) will allow it to image only ~ 5% - 10% of the celestial sphere in the energy range 0.2 - 4 keV (3Å - 60Å). This limitation would be overcome by Robisat.

The principal 80 cm aperture Wolter I telescope will provide a complete sky survey, with ~ arc minute resolution, over an energy range similar to Einstein (2 - 0.15 keV). Our proposed Soft X-ray Camera, sensitive over the range 50Å - 250Å (0.25 - 0.05 keV) would be used to extend the survey into the XUV region. The energy range extends (by a factor of ~3) and thereby complements that of HEAO-B and most other previous soft X-ray experiments. The survey nature of the experiment will allow for extensive cataloging of all types of soft X-ray sources and should result in the discovery of new classes of sources.[28,29,30] This latter point is especially true for those sources that have very soft X-ray spectra, or those that occur infrequently in nature (i.e., only a few in the galaxy), so that the survey is essential. The follow-up pointing observations will allow deeper exposures of selected fields, to improve the detection and location accuracy of sources found in the survey. These follow-up observations will also provide better data on time variability, the mapping of possible source structure and the organisation of an active guest investigator programme.

The Wide-Field Soft X-ray Camera would be mounted alongside the main Robisat telescope and would use common aspect data. The survey would be carried out by a slow rotation (~4 degrees/min) of Robisat, normally pointing towards the zenith

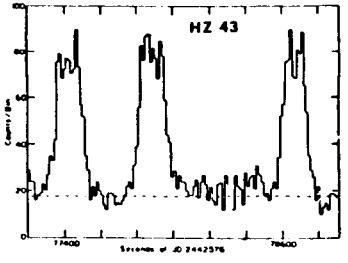

Figure 2 Discovery scans of the hot white dwarf HZ43 (44Å-80Å) made with SAS-3.[3]

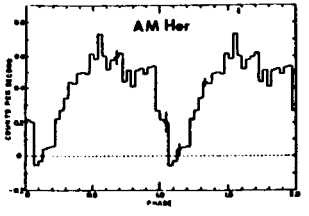

Figure 3 The 3.1 hour orbital light curve for the dwarf nova-like object AM Her, in the wavelength range 44Å-80Å (SAS-3 result[10]).

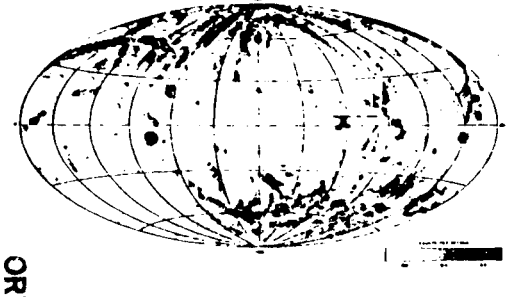

Figure 4 X-ray map of the soft x-ray background (44Å-80Å) produced from SAS-3 data.[20] The general enhancement of x-ray emission towards the galactic poles is evident. Blank areas are regions where there was no exposure. Several bright discrete sources can also be seen on the map.

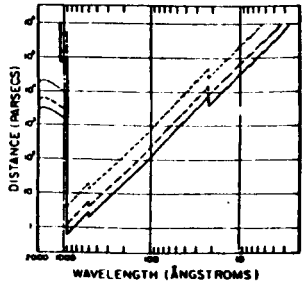

Figure 5 Distance at which the attenuation by the interstellar medium of the incident radiation reaches 90%, vs. wavelength. The three curves are for interstellar densities of 0.2, 0.1 and 0.03 cm^{-3}. (Taken from ref. 25)

and in a plane approximately perpendicular to the solar vector. Thus the Soft X-ray Camera will image a great circle 8 degrees wide every satellite orbit (~90 mins) and the whole sky in 6 months. As an example of the sensitivity of the proposed survey made, we estimate that the average exposure to a given 50-square degree field of view will be $\sim 10^4$ s. The minimum detectable source intensity for such an exposure ranges between $1-20\times10^{-11}$ ergs cm^{-2} sec^{-1} keV^{-1} in the various filter bands covering the region 50Å - 250Å (see Section 5 for detailed sensitivity calculations). This corresponds to a source with 3×10^{-4} times the intensity of HZ43. For comparison, this is near two orders of magnitude greater sensitivity than for the Berkeley Apollo-Soyuz experiment which observed only a small fraction of the sky.

During such a survey, the Wide-Field Soft X-ray Camera would yield significant results in at least six areas: (i) the study of a wide variety of stellar sources as discussed above; (ii) imaging of nearby supernova remnants, at lower energies than previously possible (e.g., the Vela supernova remnant); (iii) mapping of the ultrasoft X-ray background down to scale size of ~10'; (iv) imaging extended extragalactic objects with very low surface brightness (at high galactic latitudes); (v) study of the soft X-ray emission from some classes of compact extragalactic sources; and (vi) the discovery of new classes of X-ray objects (e.g., hot neutron stars[30], the central stars in planetary nebulae[28]) and entirely new astrophysical phenomena that have previously escaped detection because of their soft X-ray spectra or the infrequency of their appearance in nature.

Specifically, the proposed experiment will yield critical new information in several broad areas of current astrophysical research. (1) The study of very soft X-rays from stellar objects would greatly advance our understanding of such phenomena as colling mechanisms in white dwarfs[31] and neutron stars[32]; the composition and structure of the atmospheres of hot stars[33]; the temperature, emission measure and variability of stellar coronae[34]; and flare mechanisms in dwarf novae[35] and in flare stars[36]. (2) The all-sky imaging of the ultra-soft X-ray background and the supernova remnants imbedded therein will greatly contribute to our present understanding of the dynamics of the multi-temperature interstellar medium[37], the dynamics and evolution of supernova remnants[38], and the generic relation between supernova remnants and the hot component of the interstellar medium[39]. Contributions to the ultra-soft X-ray background from discrete sources[40] will be directly measured. (3) At higher galactic latitudes, soft X-rays will be detectable[25] from a variety of extragalactic objects within the observed energy range. X-ray production mechanisms in the intracluster medium within clusters of galaxies[41], and the nature of the radio lobes of active galaxies (such as Cen A[42]) will be investigated. Many compact extragalactic sources, prominent

examples of which are the BL Lac object Mkn 421[10], which exhibits copious soft x-radiation, and the QSO 3C273[43], show no apparent intrinsic spectral cut off at soft X-ray wavelengths. Observations in this energy range may ultimely be crucial to our understanding of these sources.

It is a truism in astronomy that whenever a new wavelength band is thoroughly explored, new astrophysical phenomena are discovered. The limited studies of the sky in the wavelength interval $15\text{Å} < \lambda < 80\text{Å}$ to date have already shed much new light on a wide range of astrophysical phenomena, as described above. (It is interesting, for example, to note that X-ray emission from the Cygnus Loop or HZ43 would not have been discovered without studies in this wavelength range.) For many cosmic objects with plasma temperatures in the range $T = 4\text{-}8 \times 10^5$ K, or black body temperatures in the range $T = 1\text{-}3 \times 10^5$ K, the sensitivity of present or previous satellite experiments is inadequate for their discovery. These temperature ranges are indicative of many interesting and important high energy astrophysical processes. It is thus entirely possible that in addition to enhancing our understanding of known astrophysical objects, entirely new phenomena will be discovered by the proposed experiment. As an example of this possibility, consider the enormous advances in astrophysics that resulted from the analogous discovery of X-ray binaries[44] with the first astronomy satellite (Uhuru) to explore an adjacent (2 - 10 keV) energy band.

3. Instrument Description

The wide field camera consists of three nested grazing incidence mirrors with a microchannel plate at the focal plane. The sensitive wavelength range of the present rocket experiment is 50Å - 250Å. The field of view is 8° with an angular resolution of ≈ 2' over the central 4° diameter and ~5' over the remainder of the field. Two fixed filters, dividing the focal plane, define two energy bands for crude spectral discrimination. Filters may be changed for the Robisat missions based on the experience of our rocket flights to allow for different wavelength bands, including extension to the EUV (300Å - 600Å). A schematic drawing of the wide-field camera experiment is shown in Figure 6.

a. Optics

Extensive ray tracing analyses have been carried out to determine the surface figure of the mirrors that best optimises the field of view, the angular resolution, and the effective area. We investigated the possibility of adding polynomial perturbations to standard paraboloidal/hyperboloidal surfaces. The perturbations were then numerically varied to optimise the angular resolution. The results were not significantly better than for the Wolter-Schwarzschild (W-S) design,[46] which

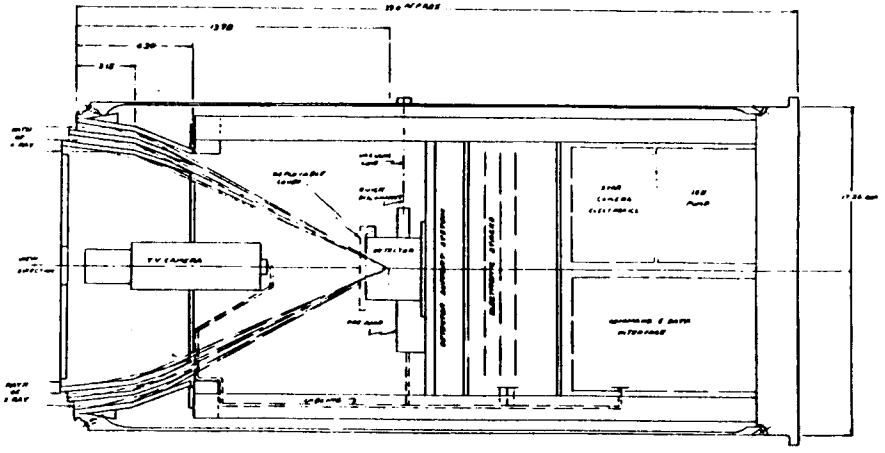

Figure 6 Schematic of the Wide-Field Soft X-Ray Camera payload. (Dimensions are in inches.)

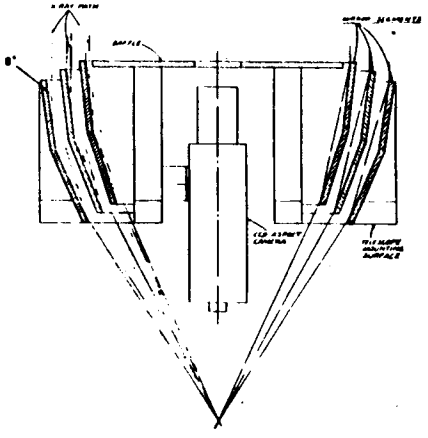

Figure 7 Schematic of the nested grazing incidence x-ray mirrors. The average grazing angle for the outer mirror is 8°.

itself is a considerable improvement over a paraboloid/hyperboloid design.[47] We have therefore adopted a W-S design.

The nested X-ray mirrors are shown in a cross-sectional schematic in Figure 7 for the Wolter-Schwarzschild design we have adopted. The effective area and angular resolution of the telescope are shown in Figure 8. For a flat focal plane detector set at the focal point for on-axis rays, the resolution (rms blur circle radius) is $<2'$ for the central 2^0 diameter and degenerates to $\sim 20'$ at the edge of the field. A flat focal plane detector can be slightly defocussed to improve the off-axis aberrations. The result is an average resolution of $\sim 8'$ over the entire field of view. A curved focal plane detector yields significantly better resolution over the entire field; $<2'$ for the central 4^0 diameter and $\sim 5'$ over the remainder of the 8^0 diameter. We intend to incorporate such a curved detector in the later 1981 rocket flights and in the Robisat instrument.

The fabrication of the X-ray mirrors for our rocket payload is nearing completion. Each mirror was machined from a solid ingot of forged aluminium. Since each mirror element is so short, it was possible to have both the first and second reflecting surfaces cut from a single block of metal. What was to be the final figure was cut on an ordinary numerically controlled lathe at Ober Tool and Dye Co., Everett, MA. Optical tests revealed the presence of low amplitude surface ripples ($\sim 3\,\mu$m, within requested tolerances) with an approximate periodicity of a few mm. These ripples resulted in an image whose rms blur circle radius is $\sim 8'$; this was judged unacceptable. In consequence MIT have contracted to have the final surface figures recut on a single-point diamond turning lathe (at Oak Ridge). This machine is capable of improving the telescope's performance by more than an order of magnitude. The mirrors are presently being plated with 0.010" of electroless Ni into which the final surface cut will be made. Once the mirror surfaces have been machined, the electroless Ni will be polished and "superpolished" (by Applied Optics Center, Burlington, MA). A film of gold will then be evaporated onto the surfaces to enhance the reflectivity in the $50\text{Å} - 250\text{Å}$ band. The X-ray reflectivity of the assembled mirror will be tested at 44Å in the 210 foot X-ray facility of AS&E. Any defects in the quality of the surface polish will be most evident at these shorter wavelengths. The reflectivity of flats, constructed by the same procedure, will be measured at several wavelengths throughout the soft X-ray and EUV region.

b. Focal Plane Detector

The imaging detector will consist of a 50 mm diameter microchannel plate in the Chevron configuration that has a $30\,\mu$ pore size. The detector itself is similar to the Leicester design on Einstein (except that it has twice the diameter). The readout scheme is, however, considerably simplified over the Einstein scheme.[48]

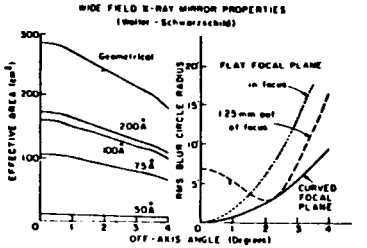

Figure 8 Properties of the wide-field Wolter-Schwarzschild x-ray mirrors. The effective area of the mirrors and off-axis resolutions are shown as a function of the off-axis angle.

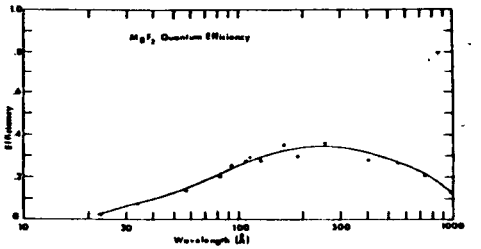

Figure 10 Photoelectric yield vs. wavelength for MgF_2 at 30^0 glancing angle. The curve is synthesized from the data in references 52, 53 and 54.

Figure 9 The 0.4m diameter x-ray mirrors used in our x-ray astronomy sounding rocket program to produce the images shown in Figure 1.

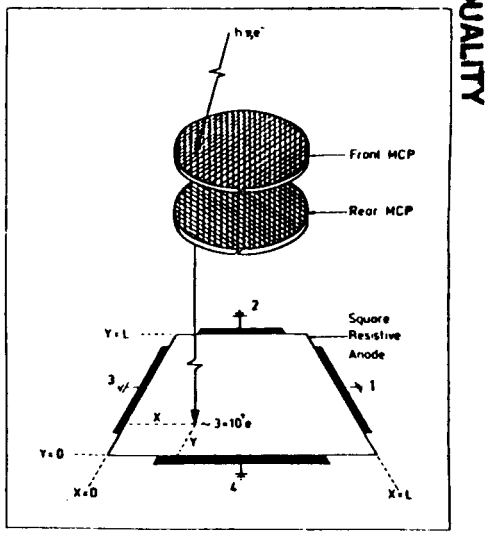

Figure 11 Schematic of the micro-channel plate detector and resistive sheet readout.

Soft X-rays that strike the face of the detector liberate a photoelectron from the MgF_2 coating. The efficiency for this conversion with X-rays incident at 30° is shown in Figure 10. Electrons are multiplied as they are accelerated through the pore with a voltage of ~1500 V on each of the two stages of the detector. The device is operated near saturation with a total gain of $\sim 4 \times 10^7$. The electron cloud then impinges on a resistive sheet which has a preamplifier coupled to each of its four edges (Figure 11). The centroid of the electron cloud is determined via charge ratio circuits to an accuracy of ~ 50 μ ; this corresponds to an angular resolution of ~30 arcsec.

A photograph of a working laboratory model of the instrument, utilizing this type of readout, is shown in Figure 12. The flight detector for the first rocket flight is also now complete.

Figure 12 Working laboratory model of the microchannel plate detector (50 mm diameter active detector).

An X-ray image recorded with the laboratory device is shown in Figure 13. The x and y position of each X-ray event will thus be obtained along with its pulse height amplitude. It is well known that images produced by such readout schemes suffer from reproducible distortion which can be easily corrected during the data processing. Cosmic rays, which penetrate several pores, yield very large pulses and will be eliminated electronically. The detector is enclosed in a vacuum housing for convenience in ground tests; during the Robisat mission a motor-driven vacuum lid can be opened or closed on command.

c. Band-Pass Filters

Photon energy or wavelength discrimination over the 50 - 250 Å pass-band will be provided in our current rocket flights by two fixed filters, each covering about half of the focal plane. For the initial flights, either the filter pair Par N (4800 Å) : [Be(2500 Å) + C(800 Å)] or the pair Par N (4800 Å) : [Al(1250 Å) + C(1000 Å)] will be used. All of these filters are nearly opaque to the very intense (1-10 Rayleighs), geocoronal background radiation at 304 Å (49,50) and 584 Å (51), which would saturate the detector if not filtered. In addition, a

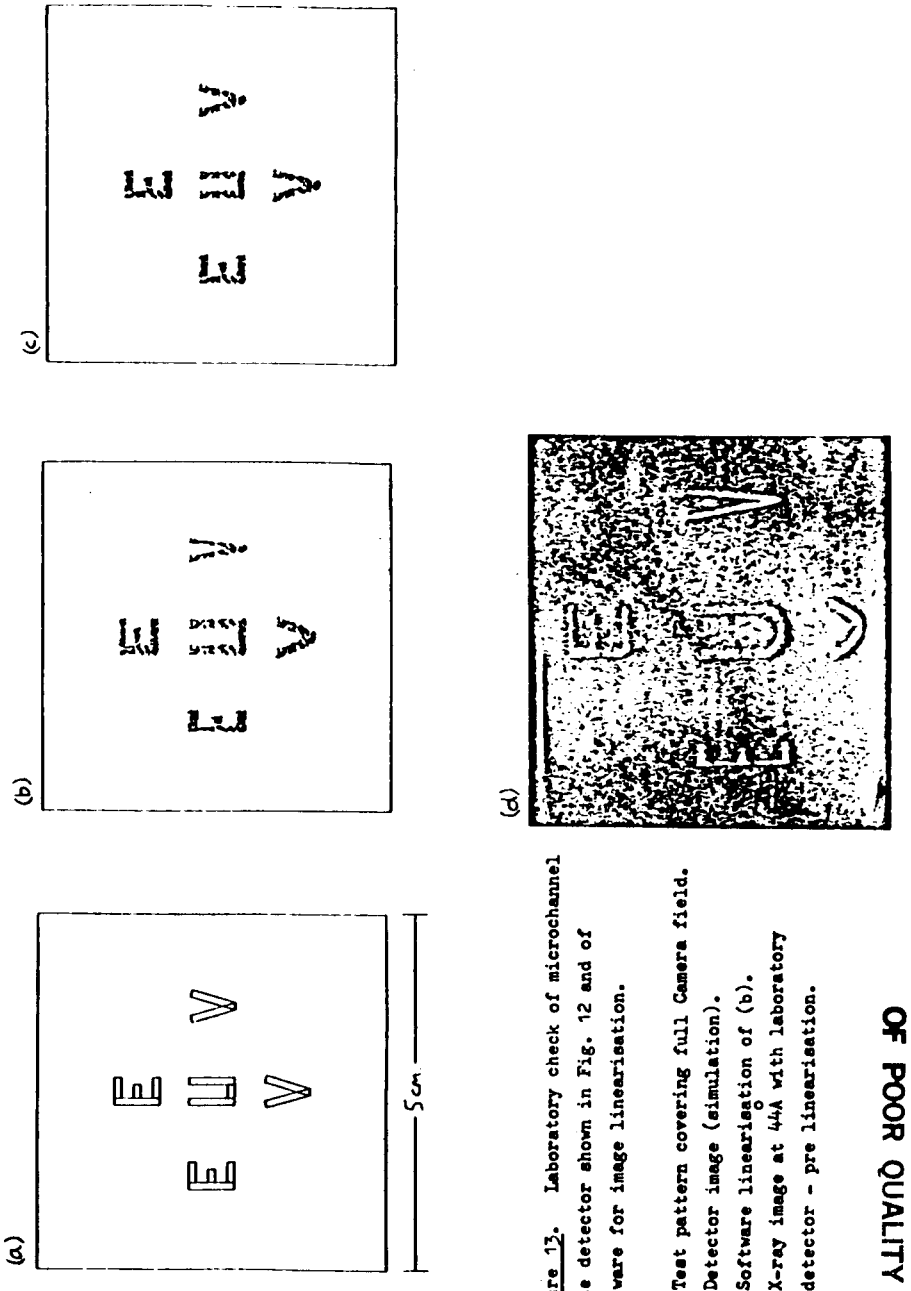

Figure 13. Laboratory check of microchannel plate detector shown in Fig. 12 and of software for image linearisation.

(a) Test pattern covering full Camera field.
(b) Detector image (simulation).
(c) Software linearisation of (b).
(d) X-ray image at 44 Å with laboratory detector - pre linearisation.

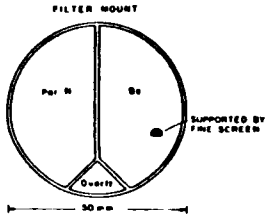

Figure 14 Schematic of the filter-mount geometry. The thin film filters are self-supporting, and are mounted on fine mesh for extra support

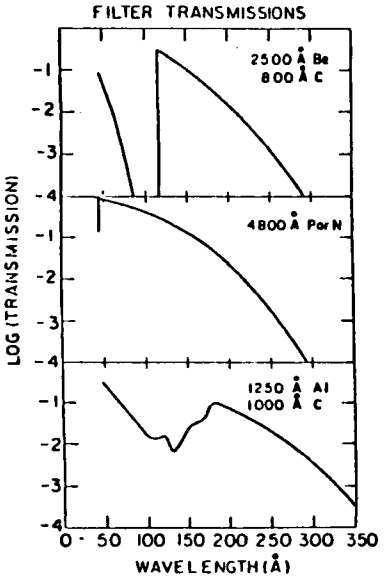

Figure 15 Transmission of the thin-film x-ray filters vs. wavelength.

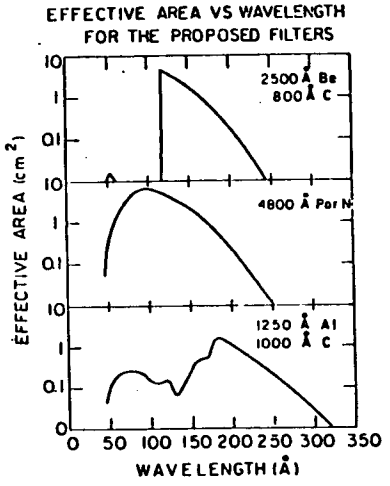

Figure 16 Effective area of the Wide-Field Soft X-Ray Camera vs. wavelength for each of three filters. These areas include the reflectivity of the x-ray mirrors, transmission of the filters, and the efficiency of microchannel plate detector.

small quartz filter in the focal plane would provide background information on cosmic ray and dark-current events, as well as on stellar UV leakage (>2000Å). The current filter-mount geometry is shown in Figure 14. The filter mount will be located as close as possible to the surface of the microchannel plate, to reduce mixed filter images on the detector. This requirement has caused some design difficulties, which have been resolved for the first rocket flight with the loss of ~1/2° at the edge of the detector field of view. The filters will be located ~0.75 cm from the detector surface. In future flights the full 8° diameter will be restored.

The transmissions of the proposed filters are given in Figure 15. The Be (115Å - 180Å) and Par N (55Å - 180Å) pair have similar long wavelength cutoffs while the different short wavelength cutoffs provide crude energy discrimination. The Par N and Al+C (150Å - 250Å) pair would provide nearly orthogonal band passes; however, the geocoronal leakage into the Al+C filter will be higher. The filters are self-supporting, but they are extremely fragile and consequently difficult to handle. Because they are so fragile, they will be reinforced in two ways. The metallic filters will be sandwiched between a fine nickel mesh and a thin (~800Å) layer of Parylene N. (The Par N filter will be supported by mesh only). These materials will significantly strengthen the filters without loss of transmission efficiency (< 30% loss). In addition, the Par N will act as a substrate for the metal foils; should any cracks develop in the filter, the Par N layer will inhibit growth of the crack and prevent the foil from shredding.

The effective detection area of the soft X-ray camera vs. wavelength is shown in Figure 16, for each of the three principal filters. These areas include the effects of the geometrical area and reflectivity of the mirrors, the transmission of the filters, and the quantum efficiency of the microchannel plate.

For Robisat the baseline design again uses fixed filters. However, it is our intention to study a simple rotating filter wheel during phase B, with possibly 5 filters, each 50 mm in diameter. These could, for instance, be chosen to extend the instrument sensitivity into the deep EUV (300 - 600Å). The mirrors and detector would work efficiently over this range, but we consider this waveband more doubtful at present, because of (i) the decreased sensitivity resulting from the intense background at 304Å [45,46] and at 584Å [47] and (ii) the lack of evidence for a class of high-energy astrophysical objects that can only be detected at wavelengths longer than 300Å.

d. Electronics and Data Handling

The signal processing electronics operate on the output charge from the microchannel plate that is collected on the resistive sheet of the detector assembl Four outputs, two x-axis outputs and two y-axis outputs, are obtained. The signal processing for one axis (x-axis) is shown in the block diagram of Figure 17. The Robisat instrument electronics is intended to follow closely the current rocket payload design. This is built and now being tested.

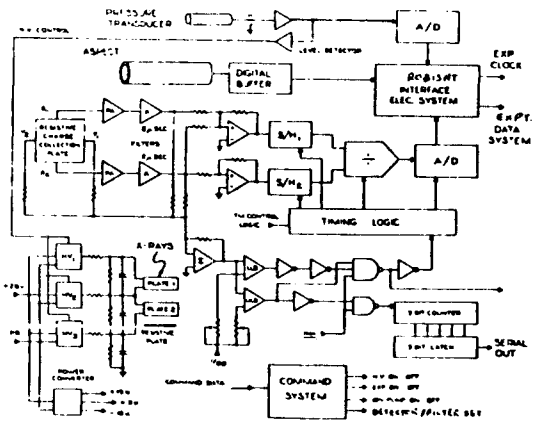

Figure 17 Block diagram of the signal processing, command, and data relay electronics.

The two x-axis outputs are first preamplified and then processed by a two microsecond active filter and amplified. The amplified x_1 and x_2 signals are then added to obtain $x_1 + x_2$. This sum is then devided into x_1 using an analog divider to arrive at the function $x_1/(x_1+x_2)$. This value represents the x position on the resistive sheet where the charge cloud from the microchannel plate was deposited. (The two y-axis outputs are processed in a like manner.) This analogue position signal is then A to D converted to a nine bit digital value and formated for presentation to the Robisat data system. In addition to determining the x and y position of the deposited charge on the resistive sheet, all four outputs from the x and y are summed together to supply a total charge value. This pulse amplitude is used to discriminate against very high and very low "energy" events. This signal is also used to initiate the timing pulses for the signal processing electronics.

A recorded X-ray event will consist of a 9-bit x-position, and 9-bit y-position with the time of each X-ray event given by its place in the recorded data stream to ~ 10 msec. Each X-ray event is processed by the detector electronics in 0.1 msec thereby yielding a maximum rate of 10^4 events s^{-1}. However, the tape recorder capacity introduces an effective limit to the recorded event rate of ~200 events s^{-1} We note that the count rate due to the brightest known soft X-ray source, HZ43, will not be significant in comparison with this maximum count rate.

A modest command system of ten discrete commands is envisaged. These commands will be operated infrequently from the ground control centre and only after some near real time data evaluation. A list of the expected commands follows:

Command	Function
1-2	Experiment on/off
3-6	Detector/filter settings
7-8	Protective cover open/closed
9-10	Ion pump on/off

The implementation of the command system and details of the power supply arrangements will be decided after further discussion with the Robisat project. No problems are envisaged.

e. Mechanical

It is anticipated that the Wide Field Camera will be mounted on the main Robisat support frame alongside and viewing parallel to the 80 cm telescope. A detailed mechanical interface would be determined during the Phase B study. This will be as simple as possible so that the camera may be constructed and tested as an independent unit. The general mechanical design will be similar to the present rocket instrument, with several obvious exceptions, as follows:

(1) a tripod-type support holds the camera into the main Robisat support frame.

(2) battery boxes will be replaced by Command and Data Interface (including the experiment tape recorder);

(3) passive thermal insulation will be provided to enclose the camera except for the open viewing areas. A design study will be made to select the required properties of the Multi Layer Insulation (MLI) to balance the heat flow from the internal electronics, from the open areas, and through the MLI itself.

In addition, the Phase B study will consider the inclusion of a simple filter wheel and the deployment of two (redundant) detector assemblies.

4. Data Analysis and Reduction

The data rate* from the Wide-Field Soft X-ray Camera will be ~3.6 K bits s^{-1}. The data consists of camera-centered positions for up to 200 individual soft X-ray photon events s^{-1}. In addition there will be the satellite aspect data. At this data rate, some 2-3 magnetic tapes per day are required to store the data. For a two year mission this corresponds to ~700-1000 magnetic tapes.

* This assumes inclusion of a second 300 Mbit capacity tape recorder. Only ~300 bits s^{-1} will be available from the existing Robisat tape recorder.

The analysis will consist basically of using the aspect data to compute the x-y camera coordinates of each soft X-ray photon, and placing the event in a bin on the celestial sphere. The basic algorithms for producing X-ray images from data acquired with a moving telescope, as well as smoothing and filtering algorithms have already been developed for our sounding rocket programme and the Einstein Observatory analysis at Leicester. We plan to develop much of the remaining necessary analysis software for our sounding rocket programme involving the Wide-Field Soft X-ray Camera.

Picture processing for the case when the satellite has a fixed or nearly fixed orientation is relatively simple. For a 1' pixel size there are only $\sim 4 \times 10^5$ pixels within or near the field of view. Each photon will be assigned a pixel and the image will be built up on the computer disk. For data acquired while the Orbiter is rotating, the 8°-wide band around the sky would be divided up into 10^6 three-arc-min-bins. The imaging would then proceed in the same manner as for the pointed observations. A second pass through the data could then be made to locate the detected sources more precisely. Imaging of large diffuse objects will not require finer pixels.

5. Results Expected

The results of the flight of the Soft X-ray Camera on Robisat will include an all-sky survey in the wavelength range 50Å - 250Å. The exposure times for the 8° field of the X-ray camera will range from hundreds of seconds to hours with an average of $\sim 10^4$ s per field. The potential importance of the survey lies in the exploration of a largely unstudied wavelength band, but with the knowledge that there are many known sources in the immediately adjacent soft X-ray band (10Å - 80Å). To understand the power of the proposed survey we must first estimate the sensitivity of the experiment for detecting several types of objects: (i) point sources against an apparently diffuse background; (ii) extended but finite size sources (e.g., supernova remnants or clusters of galaxies ($\sim 10'$ to $\sim 4°$) that appear against a diffuse background; and (iii) the diffuse background itself.

The sensitivity calculations start with an estimate of the background counting rates. There are contributions from four sources: (i) detector dark current ($\sim \frac{1}{2}$ cnt cm^{-2} s^{-1}); (ii) non-rejected cosmic ray and atmospheric γ-ray background ($\sim \frac{1}{4}$ cnt cm^{-2} s^{-1}); (iii) the ultrasoft X-ray background (the empirical formula $N(E) = 2 \times 10^4 E^{-1} \exp(-E/25 \text{ ev})$ ph cm^{-2} s^{-1} sr^{-1} eV^{-1} accounts for the measurements of Cash et al. and Levine et al. (see Figure 18) in the wavelength range ~ 80Å - 140Å, and also allows for a very rapidly rising spectrum towards lower energies); (iv) geocoronal lines (~10 Rayleighs at λ304Å and λ584Å; 10kR at λ1216Å).

For a source that yields s counts per pixel, and an average of b background counts per pixel, we define the significance of the detection to be $\sigma = s/(s+b)^{\frac{1}{2}}$. For the case where $b \ll s$, $\sigma = s^{\frac{1}{2}}$, which is the rms error in the determination of the source intensity. When $b \gg s \gg 1$, then $\sigma = s/b^{\frac{1}{2}}$; σ is then the statistical significance for the existence of the source. When b and s are both small numbers (i.e., $\lesssim 50$), the proper evaluation of a confidence limit requires Poisson statistics. In all of these cases, the requirement that $\sigma = 5$, insures a meaningful detection (e.g. a minimum of 25 source counts for the low background case, and a 5σ detection in the limit of Gaussian statistics).

The minimum detectable source intensity S_{min} (ergs cm^{-2} s^{-1} keV^{-1}), in the energy band of interest, is calculated as follows. Let $s = SAT\Delta E$ where $A\Delta E$ is the effective area x energy band ("grasp") of the instrument (properly computed for a range of spectra) and T is the exposure time. The background counts b equal $BT\theta^2$, where θ is the angular extent of a pixel (~2 times the rms blur circle radius). We then find:

$$S_{min} = \left(\frac{E_o}{100 \text{ eV}}\right) \frac{\sigma^2}{2AT\Delta E} \left[1 + \sqrt{1 + \frac{4B\theta^2 T}{\sigma^2}}\right] 1.6 \times 10^{-10} \text{ erg cm}^{-2} \text{ s}^{-1} \text{ keV}^{-1}$$

Here B is computed from the four background rates discussed above in units of counts s^{-1} sr^{-1} (integrated over the energy band of interest), and E_o is the centre of the filter band. The cosmic ray and dark current rates have been put into the same units for convenience. For the Par N and Be filters, the expected value of B is ~ 3000 s^{-1} sr^{-1}. The background rate several times greater in the Al+C filter. The minimum detectable point source intensity vs. exposure for the Par N filter is plotted, as an example, in Figure 19a, for a range of possible angular resolutions. The curves marked "flat" and "curved" focal plane detectors reflect the expected sensitivities for these two cases. We plan to use a curved focal plane detector because of the factor of ~2 improvement in sensitivity for exposure times of $\gtrsim 1000$ For a fixed angular resolution of ~5' (rms blur circle radius) we show in Figure 19 the minimum detectable source intensity vs. exposure for a range of possible background rates (Par N filter).

The average point source sensitivities which should be achieved over most of the celestial sphere during a 6 months survey mission are 0.3, 1, 7×10^{-11} ergs cm^{-2} s^{-1} keV^{-1} in the wavelength bands 55Å - 180Å, 115Å - 185Å, and 150Å - 225Å, respectively. If we use HZ43 as a standard of intensity (I_o), then our survey will yield 4×10^{-4} I_o and 10^{-4} I_o in 10^4 and 10^5 s exposures, respectively, in the region 55Å - 180Å. This sensitivity is at least comparable to that of the Berkele EUVE Explorer and more than 100 times as sensitive as the Berkeley Apollo-Soyuz experiment in the overlapping wavelength bands. The sensitivity is more difficult to compare with HEAO-1 and the Einstein Observatory because the energy ranges

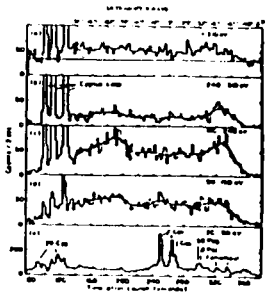

Figure 18 Ultrasoft x-ray counting rate data in several bands covering the range 40Å-140Å obtained during a sounding rocket flight.[18] The field of view of the non-imaging x-ray collector was 6° (diameter) and the effective area was ~4 times that of the proposed Wide-Field Soft X-ray Camera at 100 Å.

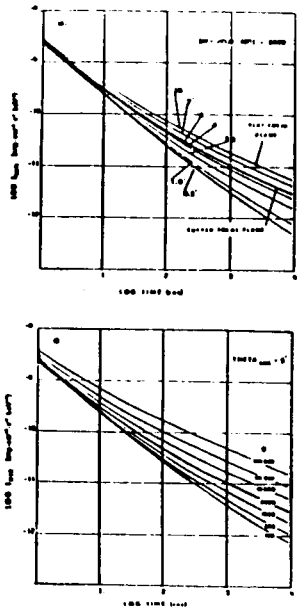

Figure 19 Sensitivity vs. exposure for (a) a range of angular resolutions and (b) a range of background rates. The heavy curve in (a) is for a Par N filter with a curved focal plane detector. The heavy curve in (b) is for the background rate expected with the Par N filter. Background units are counts s^{-1} sr^{-1}.

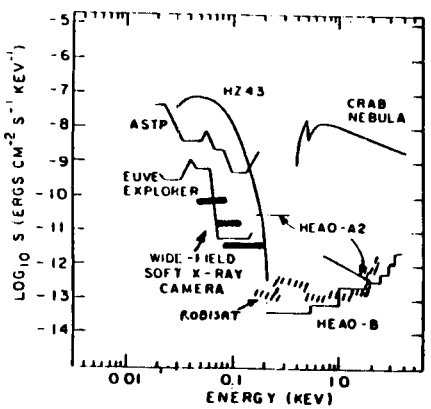

Figure 20 Comparative sensitivities among various x-ray experiments: ASTP (Apollo-Soyuz Test Project, July 1975), EUVE Explorer (scheduled for FY 1980 start(?)), A2 experiment on HEAO-1 (launched on Aug. 12, 1977), and a 3000 s exposure with the Einstein Observatory. Sensitivities of the main Robisat telescope and the proposed Wide Field Soft X-Ray Camera, in several energy bands, are shown with hatched bars (10000s exposure assumed). The spectrum of HZ43[4], the standard of intensity for very soft x-ray sources, is shown for comparison.

overlap only marginally. However, if we compare minimum detectable signals in neighbouring energy bands for the A2 experiment of HEAO-1 (all-sky) and a one hour exposure with Einstein, then we find that our sensitivity is superior to that of HEAO-1 and ~1/100 that of Einstein. These comparisons are summarised in Figure 20, which also shows an estimated survey sensitivity for the main Robisat X-ray telescope.

For diffuse objects, estimates of minimum detectable source intensities follow from the above calculations for point sources, with two differences. First, the background (i.e. events that are not from the object of interest) is more difficult to ascertain. In the case of objects smaller than the field of view, background may be obtained from the intensity surrounding the image, under the assumption that the background does not vary on scale sizes smaller than the field of view. Secondly, the resolution of the instrument must be replaced by a pixel size, which is set by the limited counting statistics, and is likely to be greater than the actual instrument resolution. The proposed wide-field camera is therefore more sensitive to diffuse objects than a small-field telescope with far superior angular resolution and comparable area. In this case, the wide field of view is more important than angular resolution.

The diffuse X-ray background itself can be mapped if the contribution of the non-X-ray background is small or if it can be determined accurately. For the Par N and Be filters, the contribution from geocoronal lines is expected to be small. The quartz filter will provide a measure of the non-X-ray background and permit a high-resolution (~10' - 30') map of the ultrasoft X-ray background to be made with about 10-100 events per pixel. We note, for comparison, that the pixel size and counting statistics for the background map would be comparable to those on our image of the Cygnus Loop (Figure 1).

The results of flying the Soft X-ray Camera on Robisat would be a sensitive and comprehensive all-sky survey in the wavelength range 50Å - 250Å. These results will complement those of the principal Robisat telescope and also the proposed Berkeley EUVE Explorer mission which extends to even longer wavelengths. The Wide-Field Soft X-ray Camera would produce important astrophysical results in six areas: (i) the study of a wide variety of stellar sources; (ii) imaging of nearby supernova remnants, at lower energies than previously possible; (iii) mapping of the ultrasoft X-ray background down to scale size of ~10'; (iv) imaging extended extragalactic objects with very low surface brightness (at high galactic latitudes); (v) study of the soft X-ray emission from some classes of compact extragalactic sources; and (vi) the discovery of new classes of X-ray objects.

The results would be presented as ~ 500-1000 "plates" of the sky in each of several energy bands. In addition to detailed analyses and publications on individual sources and regions, the data could be distributed as photographic images of the fields produced from a display screen, with coordinate overlays. Supplementary numerical maps would also be made available. We anticipate that many thousands of soft X-ray sources, both galactic and extragalactic, will be detected. These sources will comprise both newly discovered and known classes of high-energy astrophysical objects. The positional accuracy for point objects is 1' which is probably adequate to allow for many identifications, as has been demonstrated by SAS-3 positions for harder X-ray sources[55]. Extended objects such as supernova remnants and active galaxies will be presented as separate images with known field sources subtracted. An all-sky map of the diffuse X-ray background in this soft X-ray band will be presented in 10' angular bins.

6. Technical Summary

a. Spacecraft. Two phase A studies have been carried out by MBB and Dornier. Competitive phase B studies will begin in May-June and are expected to be completed by Spring 1981. The following parameters relate approximately to both studies:

overall spacecraft mass 1500 -2000 Kg
shuttle launch in ~ 1985
orbital inclination 56°, altitude ~ 400 Km
3-axis stabilation with fixed solar paddles and sun orientation within ~ 15°
attitude stabilisation by gyros to ± 1 arc min
attitude measurement by star scanner to ± 10 arc sec
spacecraft power 250 W
data storage (tape recorder) ~ 300 Mbit/day
ground control (preferred) at Weilheim

b. X-ray Telescope. This will be a 4-fold nested Wolter I design with maximum aperture of 80 cm and focal length 2.4 m. Mirrors will be of zerodur. 3 redundant position sensitive proportional counters will provide image resolution of 30 arc sec. An optical bench, sun-shade, thermal control and alignment system will be included. Mirror on-axis resolution is specified at 5 arc sec (FWHM), with a geometrical area of ~ 1250 cm^2 and field diameter ~ 2°.

c. Wide Field Soft X-ray Camera. A 3-fold nested Wolter-Schwarzchild design with maximum aperture 40 cm and focal length 35 cm. Mirrors of forged aluminium with nickel and gold coating. One (or two redundant) microchannel image tubes will provide image resolution better than 1 arc min (100 μ). Mirror resolution will be < 2 arc min for the central 4° of an 8° total field (curved detector). Geometrical area on-axis ~ 300 cm^2. The external Camera parameters are as follows:

mass, including mounting structure ~ 80 Kg
alignment parallel to X-ray telescope to ≤ 1 arc min
attitude control and measurement - as main telescope
power ~ 25 W
data rate ~ 3000 bits/s into WFSXC tape recorder